AD-A060 624 DELAWARE UNIV NEWARK DEPT OF MECHANICAL AND AEROSPA--ETC F/G 13/5
THE ANALYSIS AND DESIGN OF COMPOSITE MATERIAL BONDED JOINTS.(U)
JUL 78 W J RENTON, D L FLAGGS, J R VINSON AFOSR-74-2739

UNCLASSIFIED MAE-TR-215 AFOSR-TR-78-1371 NL

| OF |
AD A
060624

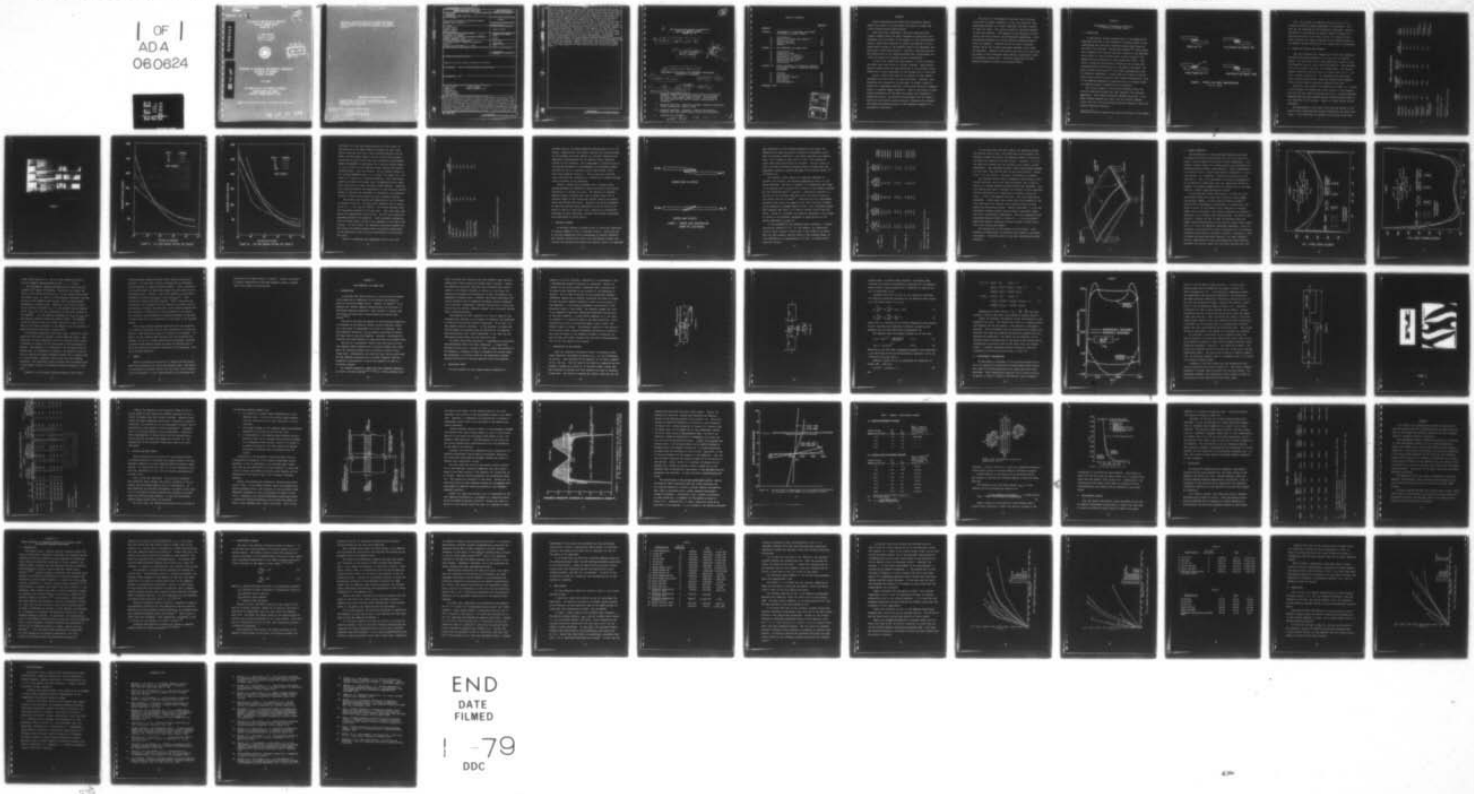

END
DATE
FILMED
1 -79
DDC

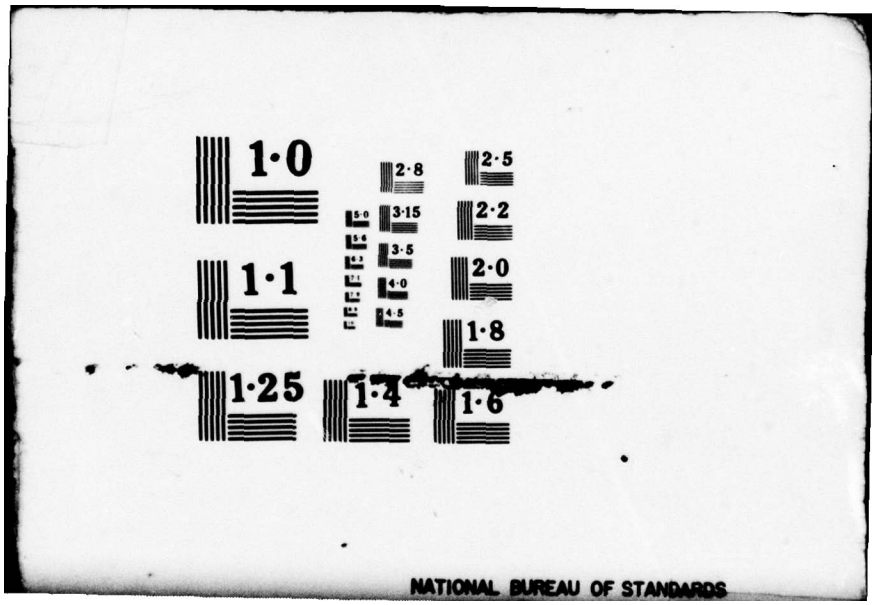
1·0
1·1
1·25
2·8
3·15
3·5
4·0
4·5
1·4
2·5
2·2
2·0
1·8
1·6
NATIONAL BUREAU OF STANDARDS

MAE TR No. 215

AFOSR-TR- 78-1371

THE ANALYSIS AND DESIGN OF COMPOSITE MATERIAL BONDED JOINTS
REPORT NO. 3

W. James Renton
Donald L. Flaggs
Jack R. Vinson

DEPARTMENT OF MECHANICAL AND AEROSPACE ENGINEERING
UNIVERSITY OF DELAWARE
NEWARK, DELAWARE

July 1978

AIR FORCE OFFICE OF SCIENTIFIC RESEARCH
UNITED STATES AIR FORCE
CONTRACT NUMBER AFOSR-74-2739

Qualified requestors may obtain additional copies from the Defense Documentation Center, all others should apply to the National Technical Information Service

Conditions of Reproduction

Reproduction, translation, publication, use and disposal in whole or in part by or for the United States Government is permitted.

AIR FORCE OFFICE OF SCIENTIFIC RESEARCH (AFSC)
NOTICE OF TRANSMITTAL TO DDC
This technical report has been reviewed and is approved for public release IAW AFR 190-12 (7b).
Distribution is unlimited.
A. D. BLOSE
Technical Information Officer

UNCLASSIFIED
SECURITY CLASSIFICATION OF THIS PAGE (When Data Entered)

REPORT DOCUMENTATION PAGE		READ INSTRUCTIONS BEFORE COMPLETING FORM
1. REPORT NUMBER AFOSR-TR- 78 - 1371	2. GOVT ACCESSION NO.	3. RECIPIENT'S CATALOG NUMBER
4. TITLE (and Subtitle) THE ANALYSIS AND DESIGN OF COMPOSITE MATERIAL BONDED JOINTS, REPORT NO. 3		5. TYPE OF REPORT & PERIOD COVERED INTERIM 6. PERFORMING ORG. REPORT NUMBER MAE-TR-74-2739
7. AUTHOR(s) W JAMES RENTON DONALD L FLAGGS JACK R VINSON		8. CONTRACT OR GRANT NUMBER(s) AFOSR 74-2739
9. PERFORMING ORGANIZATION NAME AND ADDRESS UNIVERSITY OF DELAWARE MECHANICAL AND AEROSPACE ENGINEERING DEPARTMENT NEWARK, DELAWARE 19711		10. PROGRAM ELEMENT, PROJECT, TASK AREA & WORK UNIT NUMBERS 2307B1 61102F
11. CONTROLLING OFFICE NAME AND ADDRESS AIR FORCE OFFICE OF SCIENTIFIC RESEARCH/NA BLDG 410 BOLLING AIR FORCE BASE, D C 20332		12. REPORT DATE July 1978 13. NUMBER OF PAGES 68
14. MONITORING AGENCY NAME & ADDRESS(if different from Controlling Office)		15. SECURITY CLASS. (of this report) UNCLASSIFIED 15a. DECLASSIFICATION/DOWNGRADING SCHEDULE

16. DISTRIBUTION STATEMENT (of this Report)

Approved for public release; distribution unlimited.

17. DISTRIBUTION STATEMENT (of the abstract entered in Block 20, if different from Report)

18. SUPPLEMENTARY NOTES

19. KEY WORDS (Continue on reverse side if necessary and identify by block number)

BONDED JOINTS
ADHESIVES
SHEAR MODULUS
FATIGUE LOADING
JOINT EFFICIENCY
RESIDUAL STRAIN
HYBRID ADHEREND JOINTS

20. ABSTRACT (Continue on reverse side if necessary and identify by block number)

Recent experiments have shown that significant improvements can be made in the structural efficiency of single lap joints through several modifications. Tests have been conducted in which the adherends were linearly tapered from full panel thickness to practically zero thickness over the length of the bondline in the load direction. Further, tests were conducted to examine the effects of introducing small grooves on the adhesive side of the adherends, perpendicular to the load direction. Similarly, grooves only over the thicker half of the tapered adherend were investigated, because these grooves do introduce stress concentrations. In

DD FORM 1 JAN 73 1473

UNCLASSIFIED
SECURITY CLASSIFICATION OF THIS PAGE (When Data Entered)

each case, significant improvements in joint efficiency were made under either static or fatigue loadings. Additionally, specific observations are made pertaining to the residual strain effect due to joint fabrication on the fatigue life of strain effect due to joint fabrication on the fatigue life of the joint. Second, studies were made on the effects of using hybrid adherends and their effect on joint efficiency. Recently, much discussion has centered on the placement of several layers of Kevlar-49 or fiberglass material on the outer surface of graphite panels to improve impact resistance. What is the effect of such hybrid construction on the shear and normal joint stresses in bonded-lap joints? The effects are discussed, for the cases in which the outer hybrid layers increase or decrease the in-plane and bending stiffness matrices of the adherends compared to a non-hybrid construction. The ability of the symmetric lap shear test to characterize the true shear response of a thin film adhesive, when constrained between two "rigid" adherends, has been a source of discussion for years. This report presents a detailed analysis of this test specimen. The adequacy of the analysis is justified by the use of optical and photoelastic experiments. Optimum specimen geometry for various adhesive-adherend combinations is presented. Possible sources of error introduced through use of the various measurement systems in use today are presented. Adhesive test results from the use of this test, are shown to give consistent modulus, proportional limit and ultimate strength data. The shear properties for many promising adhesive systems are presented herein.

(2)

(6) THE ANALYSIS AND DESIGN OF COMPOSITE MATERIAL BONDED JOINTS. REPORT NO. 3*

(9) Interim rept. no. 3,

(10) W. James Renton**
Donald L. Flaggs***
Jack R. Vinson†

(15) AFOSR-74-2739

DEPARTMENT OF MECHANICAL AND AEROSPACE ENGINEERING
UNIVERSITY OF DELAWARE

(14) MAE-TR-215 (16) 2307 (17) B1

(18) AFOSR (19) TR-78-1371 (11) July 1978 (12) 69 p.

* Research sponsored by the Air Force Office of Scientific Research, Office of Aerospace Research, United States Air Force, Grant Number AFOSR-74-2739. This document has been approved for public release; distribution is unlimited.

** Research Associate; Presently, Manager, Composite Materials, Vought Corporation, Dallas, Texas.

*** Research Assistant; Presently, Research Engineering, Lockheed Palo Alto Laboratories, Palo Alto, California.

† Professor and Chairman

405 927

mt

TABLE OF CONTENTS

		Page No.
ABSTRACT		1
CHAPTER I	- IMPROVEMENT IN STRUCTURAL EFFICIENCY OF SINGLE LAP BONDED JOINTS	
A.	Introduction	3
B.	Static and Fatigue Test Results	5
C.	Residual Strains	12
D.	Hybrid Composites	18
E.	Summary	22
CHAPTER II	- THE SYMMETRIC LAP SHEAR TEST	
A.	Introduction	24
B.	Analytical Study	25
C.	Formulation of Problem	26
D.	Experimental Confirmation	30
E.	Optimum Specimen Design	36
F.	Experimental Results	45
G.	Conclusions	46
CHAPTER III	- SHEAR PROPERTIES OF PROMISING ADHESIVES FOR BONDED JOINTS IN COMPOSITE MATERIAL STRUCTURES	
A.	Abstract	48
B.	Introduction	49
C.	Experimental Program	51
D.	Test Results	54
E.	Conclusions	61
F.	Acknowledgements	63
REFERENCE LIST		64

ABSTRACT

Recent experiments have shown that significant improvements can be made in the structural efficiency of single lap joints through several modifications.

Tests have been conducted in which the adherends were linearly tapered from full panel thickness to practically zero thickness over the length of the bondline in the load direction. Further, tests were conducted to examine the effects of introducing small grooves on the adhesive side of the adherends, perpendicular to the load direction. Similarly, grooves only over the thicker half of the tapered adherend were investigated, because the grooves do introduce stress concentrations.

In each case, significant improvements in joint efficiency were made under both static or fatigue loadings. Additionally, specific observations are made pertaining to the residual strain effect due to joint fabrication on the fatigue life of the joint.

Second, studies were made on the effects of using hybrid adherends and their effect on joint efficiency. Recently, much discussion has centered on the placement of several layers of Kevlar-49 or fiberglass material, on the outer surface of graphite panels, to improve impact resistance. What is the effect of such hybrid construction on the shear and normal joint stresses in bonded-lap joints? The effects are discussed, for the cases in which the outer hybrid layers increase or decrease the in-plane and bending stiffness matrices of the adherends compared to a non-hybrid construction.

The ability of the symmetric lap shear test to characterize the true shear response of a thin film adhesive, when constrained between two "rigid" adherends, has been a source of doubt for years. This report presents a detailed analysis of this test specimen. The adequacy of the analysis is justified by the use of optical and photoelastic experiments. Optimum specimen geometry for various adhesive-adherend combinations is presented. Possible sources of error introduced through use of the various measurement systems in use today are presented. Adhesive test results from the use of this test, are shown to give consistent shear modulus, proportional limit and ultimate strength data. The shear properties for many promising adhesive systems are presented herein.

CHAPTER I

IMPROVEMENT IN STRUCTURAL EFFICIENCY OF SINGLE LAP BONDED JOINTS

A. INTRODUCTION

In lap joints, stress concentrations in the adhesive and adherends arise due to the difference in elastic moduli of the constituents and the abrupt thickness change which occurs at the ends of the overlap. Mylonas and deBruyne[1]* among others, have suggested that tapering the outer surface of the adherends would result in a more uniform state of shear stress in the adhesive while minimizing the tear stress that exists. This result is directly attributed to minimizing the in-plane and transverse strain discontinuity at the ends of the joint. Recently, Cherry and Harrison[2] have shown mathematically that for identical adherends, a linear taper will result in the adhesive shear stress attaining a near uniform distribution, while if the adherend thickness is much less than the overlap length, the adhesive tensile stresses will be negligible.

The initial segment of this report presents static and constant amplitude fatigue test data comparing four adherend geometries. The constant thickness adherend lap joint, a linearly tapered adherend lap joint, and two linearly tapered joints that are fully and partially notched (Figure 1) along the adhesive-adherend interface.

---

*References for each chapter are given at the back of this report.

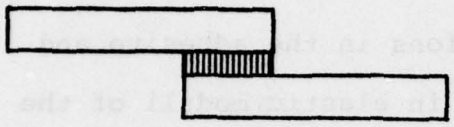

Single Lap (SL)

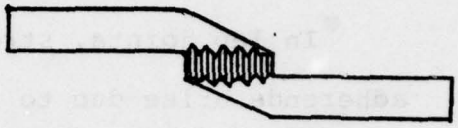

Fully Notched and Tapered (TN)

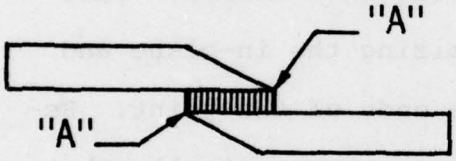

Linear-Tapered Lap (LT)

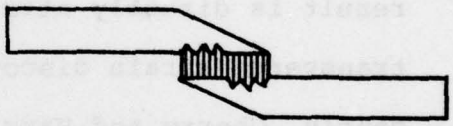

Half-Notched and Tapered (THN)

FIGURE 1. TYPICAL LAP JOINT CONFIGURATION

(not to scale)

Next, the problem of premature fatigue failure of the constant thickness aluminum adherends is investigated. Reasons for the existence of this problem are advanced. Finally, the effect of the addition of several layers of laminae of a different material to the outer surface of a composite laminated structure for impact toughness and its ensuing effect on the adhesive stress distribution of a bonded joint is discussed.

B. STATIC AND FATIGUE TEST RESULTS

The test specimens were composed of 7075-T6 bare adherends and EA951 Nylon-epoxy adhesive of .50 and .80 inch overlap length. All tests were run at room temperature, within a relative humidity range of ten to fifty-five percent. The crosshead rate for the static tests was .05 inches/minute. The fatigue results (Figures 3A and 3B) are for a stress ratio (R) of + .10 and a 30 Hertz cycling rate. All specimens were fabricated using a heated platen press, after the surfaces were prepared with a Forest Products Laboratory sulphuric acid etch.

The static test results are summarized in Table (1). Failure of the standard and tapered lap joints occurred in the adhesive. The full and half tapered specimens failed in a combined adhesive-adherend mode with the adherend usually failing along a notch at the centerline of the overlap. Figure (2) shows typical failed specimens.

Any improvement in the static load carrying ability of the various joint configurations is best reflected by its joint efficiency. Joint efficiency is defined as the ratio of the joint

TABLE 1 - STATIC TEST RESULTS

TYPE JOINT	OVERLAP LENGTH (in)	AVG. ADHESIVE THICKNESS (in)	AVG. ULT.* JOINT LOAD (lb)	JOINT EFFICIENCY (%)	TYPE FAILURE
Single Lap	.540	.0045	2600.	52.5	Adhesive
Single Lap	.800	.0055	3769.	82.5	Adhesive
Tapered	.540	.0070	2612.	52.7	Adhesive
Tapered	.730	.0020	4237.	85.0	Adhesive
Tapered and Grooved	.540	.0040	3642.	73.0	Adherend and Adhesive
Tapered and Grooved	.800	.0030	4518.	91.0	Adherend and Adhesive
Tapered, Grooved along 1/2 overlap	.800	.0070	4160.	84.0	Adherend and Adhesive

Strain Rate = .05 in/min.

Specimen Width $\cong$ 1.00"

*Average of three or more tests.

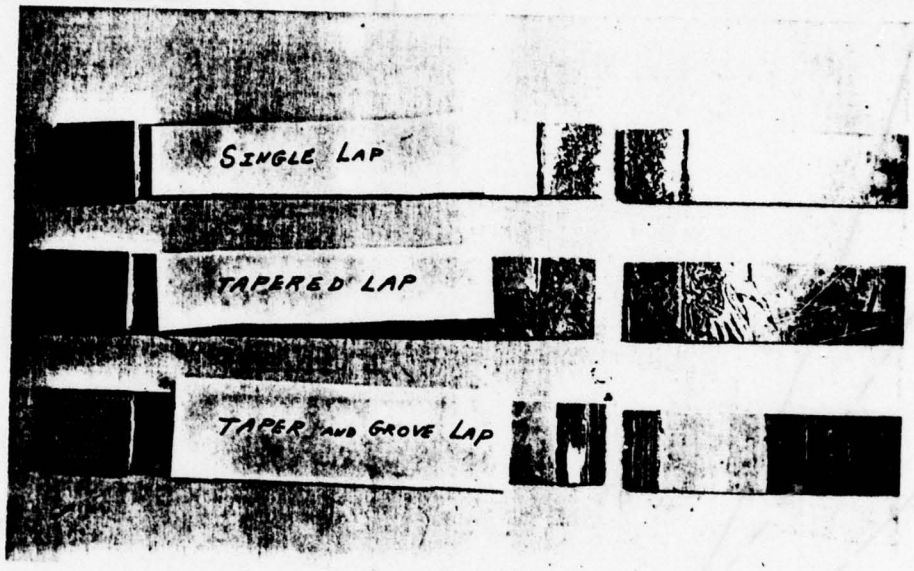

FIGURE 2

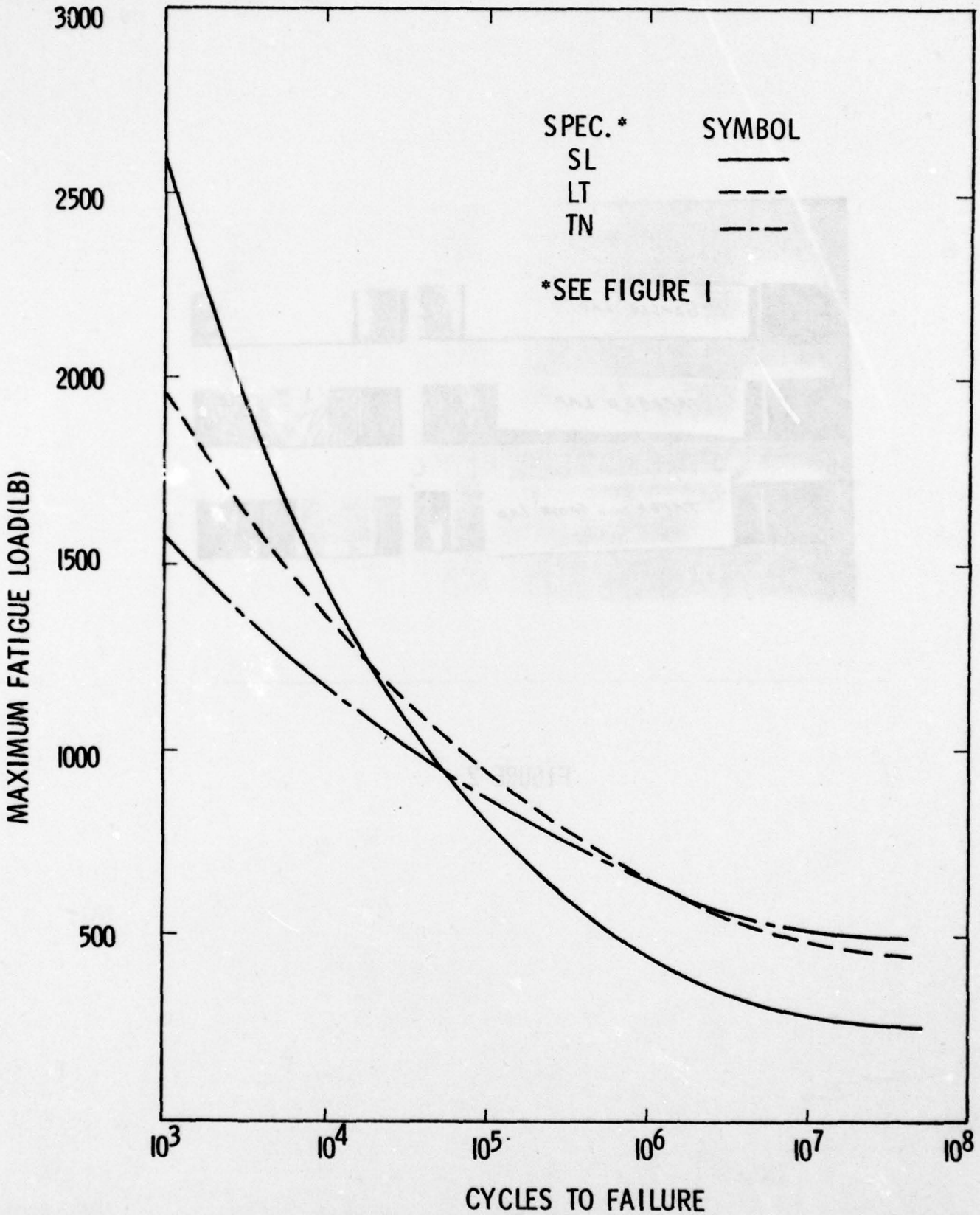

FIGURE 3A. 0.54 INCH OVERLAP FATIGUE TEST RESULTS

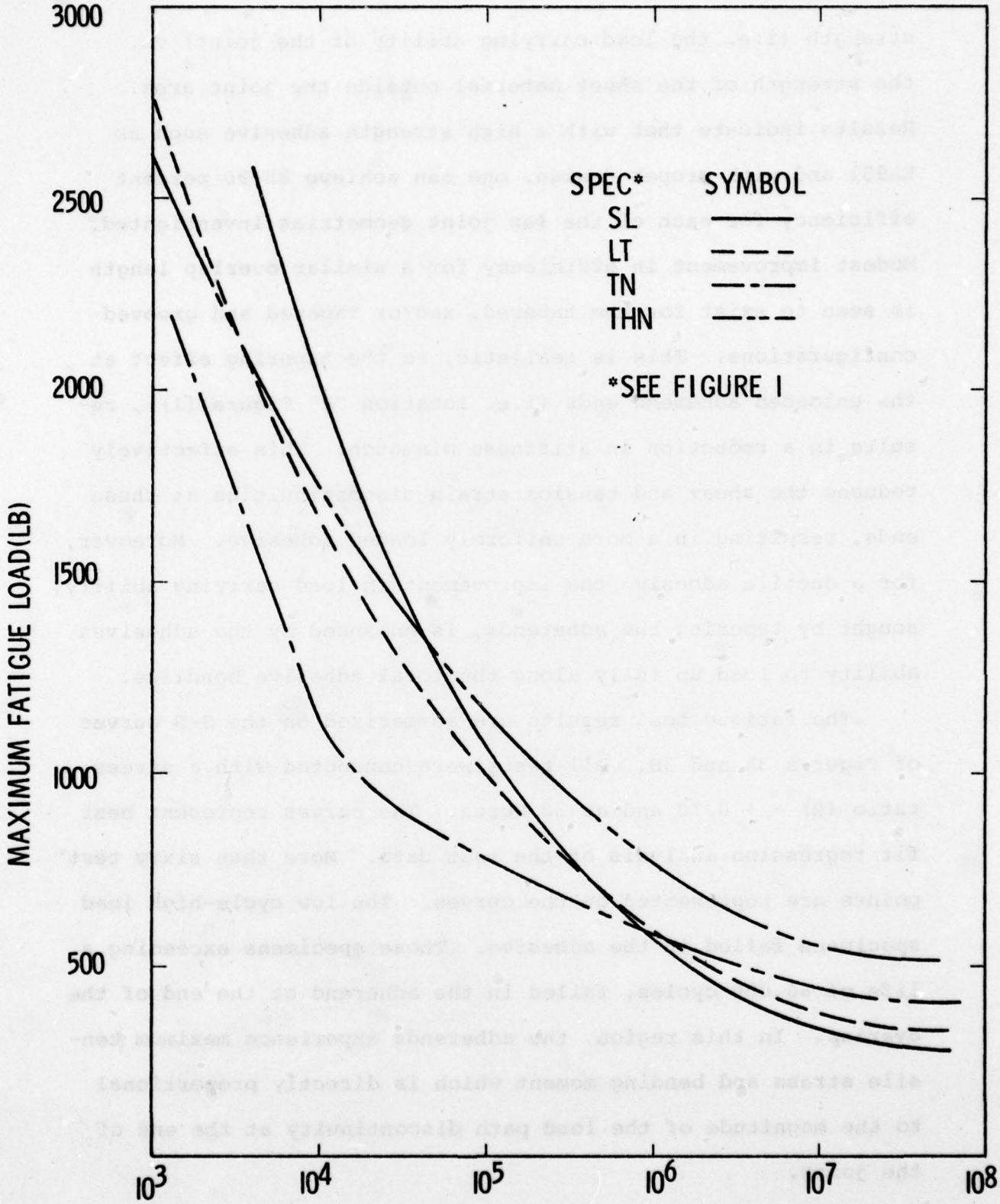

FIGURE 3B. 0.80 INCH OVERLAP FATIGUE TEST RESULTS

strength (i.e. the load carrying ability of the joint) vs. the strength of the sheet material outside the joint area. Results indicate that with a high strength adhesive such as EA951 and with proper design, one can achieve 80-90 percent efficiency for each of the lap joint geometries investigated. Modest improvement in efficiency for a similar overlap length is seen to exist for the tapered, and/or tapered and grooved configurations. This is realistic, as the tapering effect at the unloaded adherend ends (i.e. location "A" Figure (1)), results in a reduction in stiffness mismatch. This effectively reduces the shear and tension strain discontinuities at these ends, resulting in a more uniformly loaded adhesive. Moreover, for a ductile adhesive the improvement in load carrying ability, sought by tapering the adherends, is enhanced by the adhesives ability to load up fully along the total adhesive bondline.

The fatigue test results are summarized on the S-N curves of Figures 3A and 3B. All tests were conducted with a stress ratio (R) = + 0.10 and at 30 Hertz. The curves represent best fit regression analysis of the test data. More than sixty test points are represented on the curves. The low cycle-high load specimens failed in the adhesive. Those specimens exceeding a life of 80,000 cycles, failed in the adherend at the end of the overlap. In this region, the adherends experience maximum tensile stress and bending moment which is directly proportional to the magnitude of the load path discontinuity at the end of the joint.

Table (2) summarizes the improvement seen in the load

TABLE 2. SUMMARY OF FATIGUE TEST RESULTS @ 4×10^6 CYCLES

TYPE JOINT	OVERLAP LENGTH (in)	JOINT EFFICIENCY (%)
Single Lap	.540	33.5
Single Lap	.800	38.4
Tapered	.540	52.5
Tapered	.730	39.7
Tapered and Grooved	.540	52.2
Tapered and Grooved	.800	41.3
Tapered, Grooved, along 1/2 overlap	.800	54.5

R = +.10

Cycles = 30 Hz

All Failures in Adherends Adjacent to Overlap

carrying ability of tapered adherend configurations at 4×10^6 cycles. Specifically, the results indicate that the efficiency of the standard lap joint subject to a fatigue loading can be improved by approximately 20% by tapering and/or inserting grooves at the interface. This improvement is primarily due to the reduced stiffness of the adherends in the overlap region, allowing the joint to reorient itself, when loaded, into a scarf type geometry (Figure 4). This is the most efficient joint configuration, resulting in a reduction in moment and peak tensile stresses in the adherends.

Overall, results would indicate that a tapered and/or grooved specimen can definitely improve the static and fatigue efficiency of a single lap joint. The addition of properly-shaped grooves (v-notches were used in these tests) over a selected length of the overlap may further improve the joint's static and fatigue efficiency. Moreover, the proper selection of taper and grooves could conceivably allow the joint to respond to load as a true scarf joint, resulting in significant increases in joint efficiency, without the problems associated with fabrication of scarf joints.

C. RESIDUAL STRAINS

An existing problem in bonded joints of sufficient magnitude to warrant comment is that of residual strains. They arise due to the high temperature cure requirements of certain adhesives. The residual strains occur due to the differential thermal contraction and conductivity between the adhesive and/or the adherends.

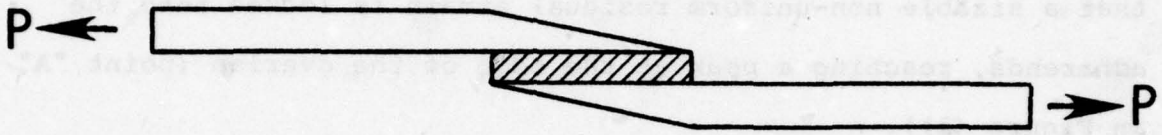

BEFORE LOAD IS APPLIED

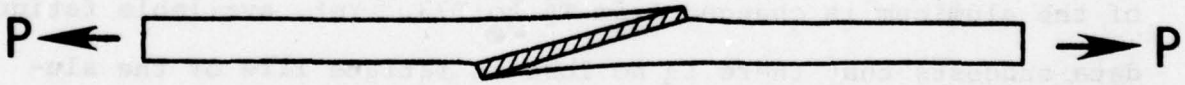

DURING LOAD PROCESS

FIGURE 4. TAPERED JOINT REORIENTATION DURING THE LOAD PROCESS

Upon completion of the elevated temperature cure cycle, the adhesive cools down and begins to acquire a significant stiffness and strength capability, long before reaching room temperature. For an adhesive that cures at 350°F, this capability occurs with some significance at 180-200°F. The net result is that a sizable non-uniform residual strain is locked into the adherends, reaching a peak at the edge of the overlap (point "A" in Figure (1)).

The residual strain effect for identical adherends is thought to be minimal, yet the data presented in Table (3) suggests otherwise. The data in columns (1-3) emphasizes that based on the applied load, and with the inclusion of the bending stresses per the Goland-Reissner[3] analysis, a significant reduction in the life of the aluminum sheet does occur for both the data in this report and that of Wang[4]. *Metallurgical* data (MIL-HDBK5A) specifies that during the adhesive cure cycle the heat treatment of the aluminum is changed from T6 to T73. Yet, available fatigue data suggests that there is no loss in fatigue life of the aluminum. Column (5) estimates the potential magnitude of the locked in stress in the adherend, necessary to cause failure at the cycles specified in column (3).

Is the magnitude of the residual strain realistic? A simple calculation suggests it is. If, for example, the temperature level at which residual strains begin to be locked in is 180°F, then the peak residual tensile strain in the aluminum sheet, at room temperature, is approximately 14.4 ksi., a sizable sum in affecting fatigue.

TABLE 3. THE INFLUENCE OF RESIDUAL STRAINS ON THE FATIGUE LIFE OF BONDED JOINTS

SPEC.	(1) MAX. SHEET STRESS (P/A + MC/1) KSI	(2) EXPECTED CYCLES TO FAILURE ($x10^6$)*	(3) ACTUAL CYCLES TO FAILURE ($x10^6$)	(4) ACTUAL MAX. SHEET STRESS FOR (3) (KSI)*	(5) RESIDUAL STRESS (4)-(1) (KSI)	TYPE OF FAILURE
.50" Single Lap	22.1	>10.0	.806	42.	19.9	Adherend
	27.6	>10.0	.668	42.	14.4	Adherend
	37.3	>10.0	.167	46.	8.7	Adherend
	64.5	.020	.012	66.	-1.5	Adhesive
.80" Single Lap	42.6	.500	.211	45.	2.4	Adherend
	57.5	.070	.053	56.	-1.5	Adhesive
	27.5	>10.0	.567	43.	15.5	Adherend
**.50" Single Lap	30.0	>10.0	.700	41.	11.0	Adherend
	44.6	.400	.200	49.	4.4	Adherend
	52.0	.100	.100	51.	-1.0	Adhesive
	25.0	>10.0	2.00	38.	13.0	Adherend

R = +.10

*Values from Goodman Curve for 7075-T6 Sheet

**From REF(4) Data - 2024-T3 Sheet

In the high load, low cycle region, the adhesive becomes the initial item to fail. For tests data in this region, the disparity between the actual and expected cycles to failure for the sheet was observed to become minimal. Therefore, it is in the high cycle regime that the residual strain effect is most detrimental. The resulting residual strain distribution throughout the sheet cross section must be self-equilibrating. Therefore, it is not uniform. The exact distribution is unknown.

The residual strain effect accompanying fabrication of dissimilar materials can be even more detrimental due to the addition of a thermal mismatch problem between the adherends. Initial efforts were made to quantify the residual strains resulting from the fabrication of a fiberglass to aluminum single lap joint. A 350°F cure adhesive was used. The effort was partly successful. Strain gages were placed along the periphery of the joint monitoring the residual strain buildup which occurred during the fabrication process. Results indicated: 1) that the transverse residual strains were an order of magnitude larger than their longitudinal counterparts. This was supported by the transverse warpage evident in Figure (5). 2) that peripheral gages were unable to quantify the peak residual strains occurring in the overlap end region.

The significance of the problem is self-evident. Yet a reliable, accurate means to resolving this problem is presently unavailable. Definitely, work in this area should prove highly rewarding.

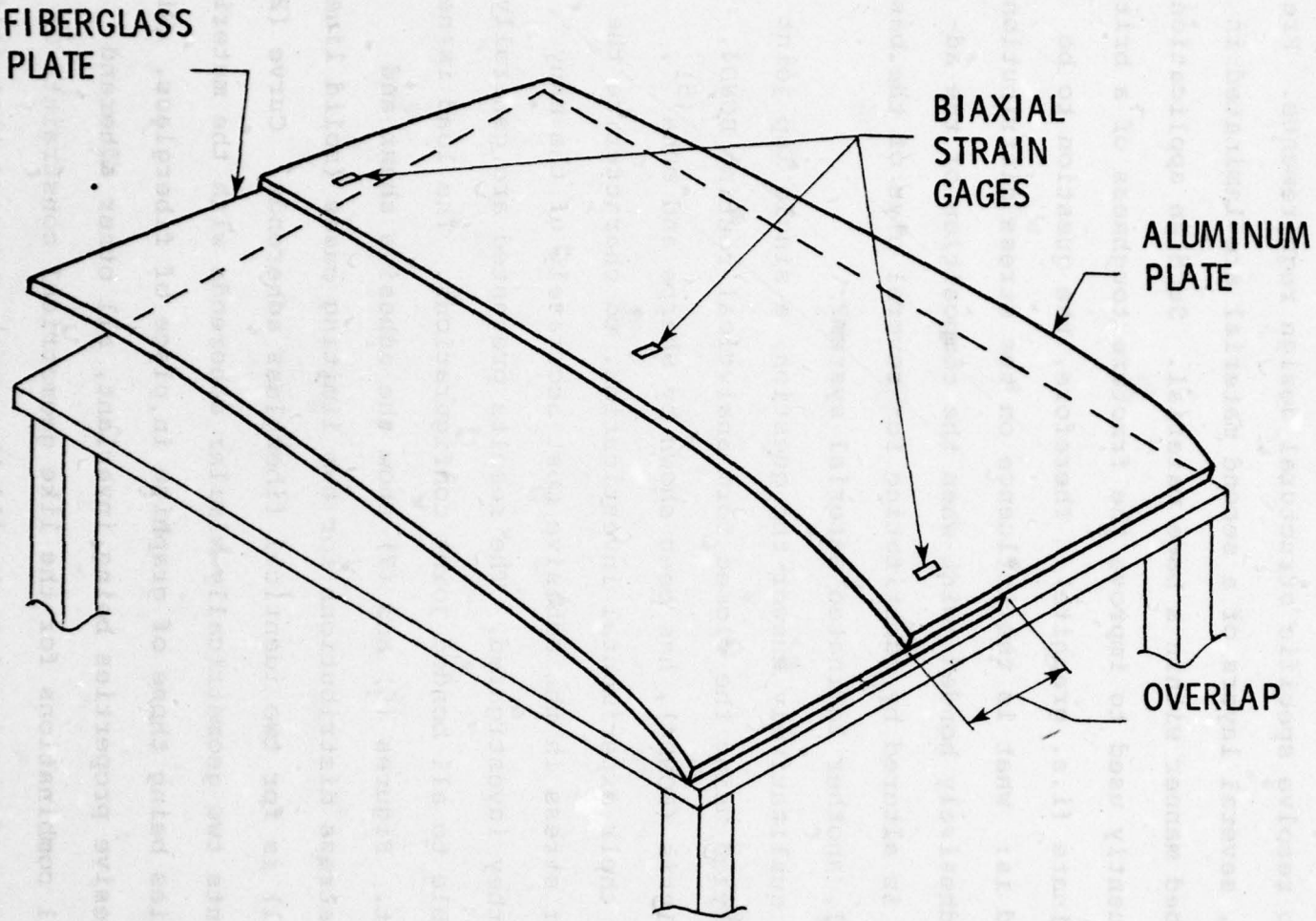

FIGURE 5. DISSIMILAR ADHERENDS WARPAGE SPECIMEN

D. HYBRID COMPOSITES

The desirability of using laminated composite materials in numerous structural applications has led to the use of hybrids to resolve specific structural design requirements. Frequently, several layers of a second material are laminated in a prescribed manner within a base material. Such an application is frequently used to improve the fracture toughness of a brittle laminate (i.e. graphite). Therefore, the question to be resolved is: what is the influence on the stress distribution in an adhesively bonded joint when the composition of the adherends is altered by substituting for several plys of the base material, another laminated material system?

To qualitatively answer the question, a single lap joint was analyzed using the closed form analytical routine BOND4. The analysis (BOND4), has been shown by Sharpe and Muha[5], through their experimental investigation, to characterize the state of stress in the adhesive most accurately of the many models they investigated. The results presented are generally applicable to all bonded joint configurations. The load is held constant. Figures (6) and (7) show the adhesive shear and normal stress distributions for two limiting cases (solid lines). Curve (1) is for two identical fiberglass adherends. Curve (2) represents two geometrically similar adherends with the material properties being those of graphite in place of fiberglass. With the adhesive properties being invariant, all other adherend material combinations for the like geometrical constraints of thickness and overlap length will have peak stresses that fall

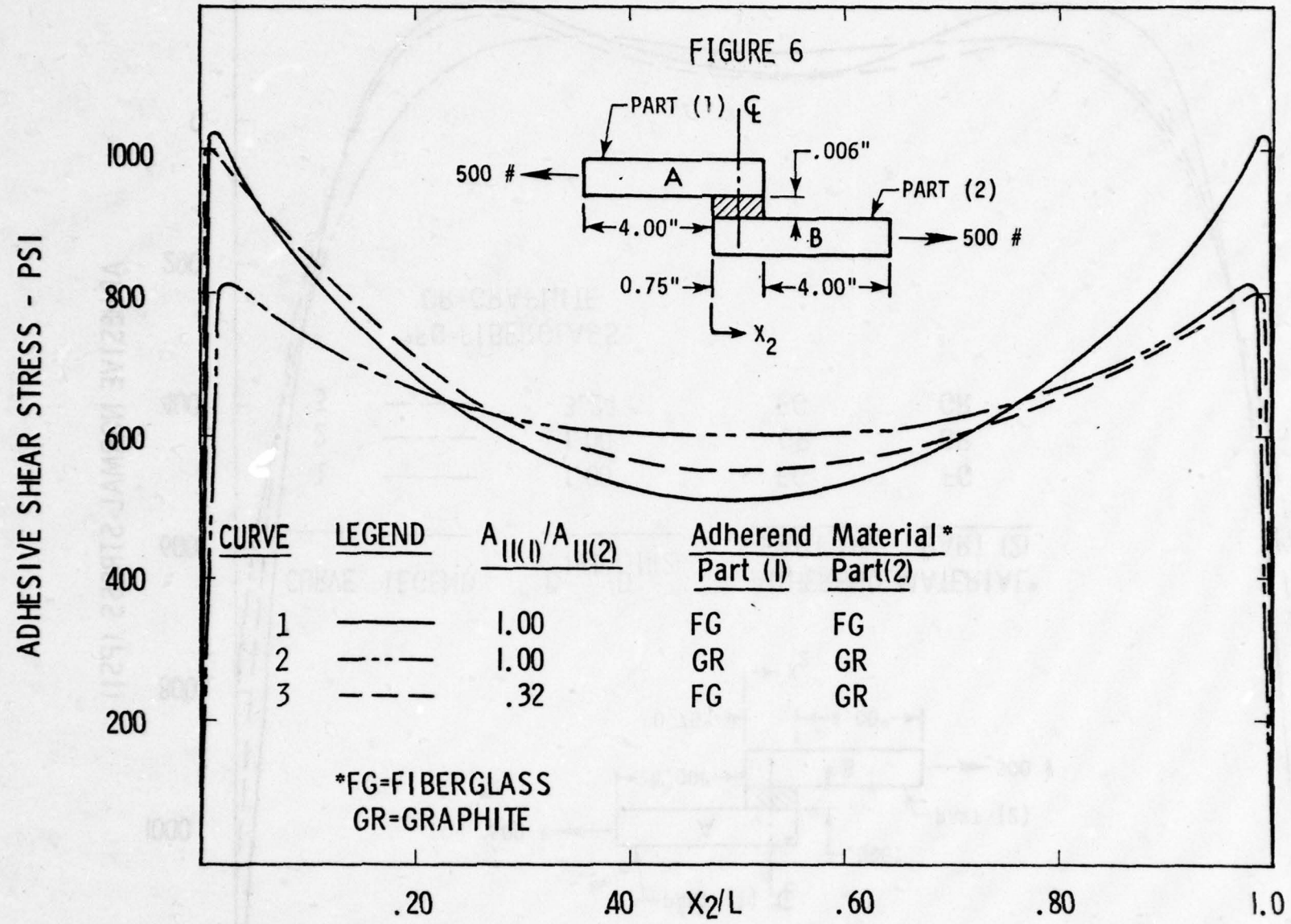
FIGURE 6
PART (1)
PART (2)
500 #
A
B
.006"
4.00"
0.75"
4.00"
500 #
X_2
ADHESIVE SHEAR STRESS - PSI
1000
800
600
400
200
CURVE
LEGEND
$A_{II(1)}/A_{II(2)}$
Adherend Material*
Part (1)
Part(2)
1
1.00
FG
FG
2
1.00
GR
GR
3
.32
FG
GR
*FG=FIBERGLASS
GR=GRAPHITE
.20
.40
X_2/L
.60
.80
1.0

FIGURE 7

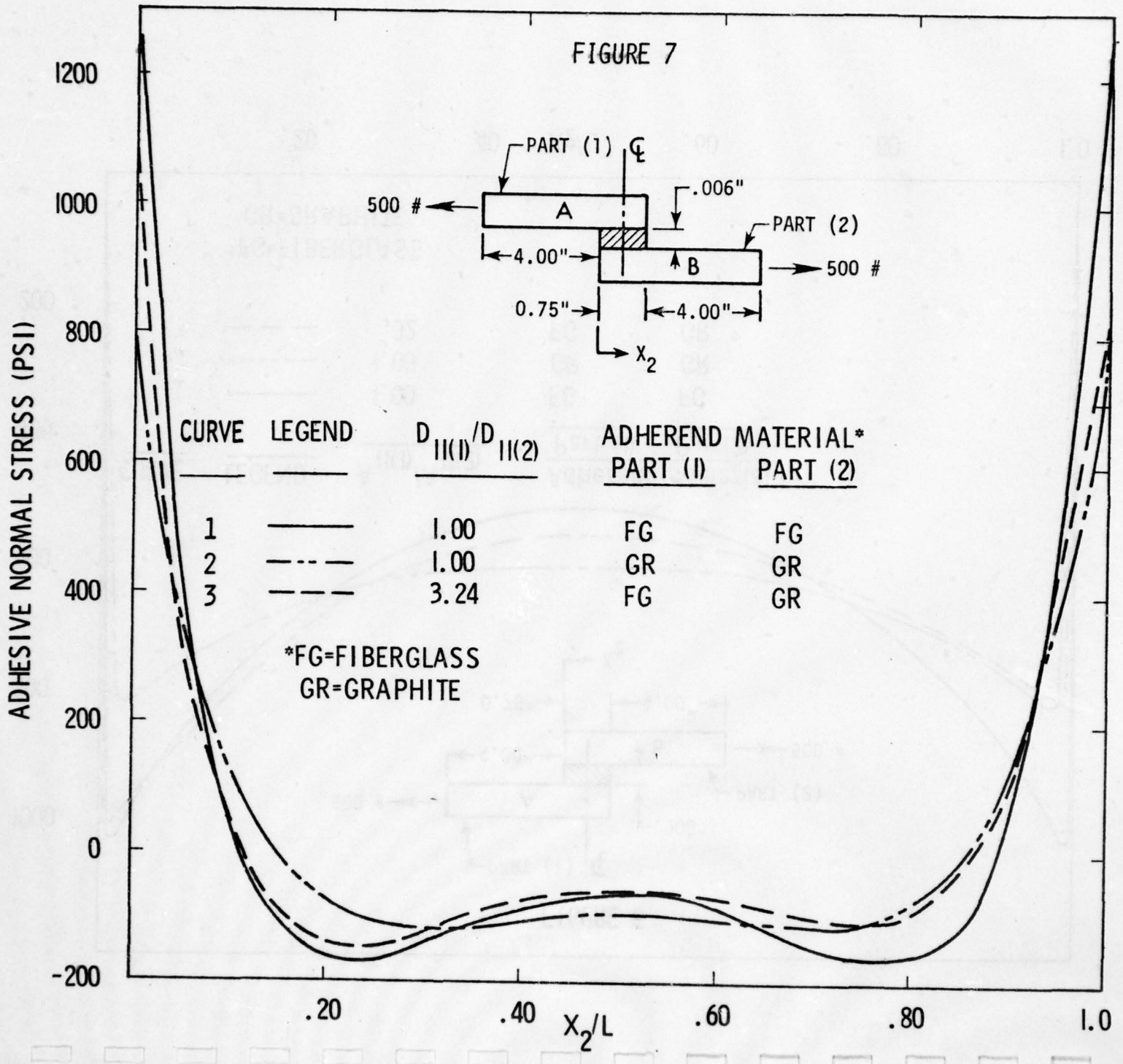
ADHESIVE NORMAL STRESS (PSI)
1200
1000
800
600
400
200
0
-200
.20
.40
.60
.80
1.0
X_2/L
PART (1)
PART (2)
500 #
A
B
.006"
4.00"
0.75"
X_2
CURVE | LEGEND | $D_{11(1)}/D_{11(2)}$ | ADHEREND MATERIAL* PART (1) | PART (2)
1 | 1.00 | FG | FG
2 | 1.00 | GR | GR
3 | 3.24 | FG | GR
*FG=FIBERGLASS
GR=GRAPHITE

within these bounds (i.e., the all glass adherend joined to the all graphite adherend shown by the — — — lines).

The fundamental adherend parameters being varied are the inplane and flexural stiffnesses. Basically, the larger the ratio of the inplane stiffness (A_{11}) to the adhesive shear modulus factor ($G_{eff} \cdot \eta$), where η is the adhesive thickness, the more uniform is the adhesive shear stress, with the stress peaks approaching a minimum value. Similarly, the larger the ratio of the flexural stiffness (D_{11}) to the adhesive tension modulus factor ($E_{eff} \cdot \eta^3$), the less significant are the peel stresses in the adhesive. η is the adhesive thickness and G_{eff} and E_{eff} are the adhesive effective shear and tension moduli. The maximum values of adhesive shear and normal stress will occur at the edge of the overlap adjacent to the adherend with the minimum inplane and flexural stiffness, respectively.

All graphite adherends, being more rigid, represent a lower bound for this study as pertains to peak adhesive stress. Substituting all glass adherends, results in the peak shear stress increasing 27 percent and the peak normal stress increasing 61 percent. The problem is to determine if by the substitution of several plys of fiberglass for graphite, the adhesive can withstand a fraction of these increased stresses for its design load vs. life spectrum, assuming a base design with all graphite laminates. The fractional stress increase would be proportional to the number of plys of fiberglass replacing graphite in each case.

Normally, an efficiently designed adhesive joint cannot

withstand these increased stress levels without failing prematurely. To avoid this, several alternatives are available to the designer to lessen the peak stresses. First, increasing the overlap length can many times reduce the peak stress to an acceptable level. Second, a less stiff adhesive can be used to increase the ratios $(A_{11}/G_{eff}\cdot\eta)$ and $(D_{11}/E_{eff}\cdot\eta^3)$. This effectively reduces the peak stresses. Third, increasing the thickness of the adherends with the addition of several plys of new material increases the pertinent ratios thereby reducing the peak stresses. Additionally, such adjustments in the design can alleviate the introduction of excessive moments at the ends of the overlap due to the insertion of the layers of the foreign lamina.

The strain mismatch problem associated with the formation of a hybrid construction has not been accounted for in this discussion. This should be a point of concern in all designs. Finally, for the instance when one must join two dissimilar adherends, the use of a hybrid design could conceivably alleviate an adverse peak adhesive stress situation by enabling one to match the inplane and flexural stiffness of the adherends. This is an optimum condition.

E. SUMMARY

Ways to increase the efficiency of adhesive bonded joints have been ascertained for static and fatigue loads. The effect of incorporating residual strains into the joint during fabrication was discussed. A full understanding of the magnitude and

distribution of these strains is lacking. Finally, the effect of hybrid construction on the peak adhesive stress in bonded joints was looked at qualitatively.

CHAPTER II

THE SYMMETRIC LAP SHEAR TEST

A. INTRODUCTION

It has been the usual practice to utilize the bulk mechanical properties of adhesives in the analysis and design of metal or non-metal bonded joints. However, as Zabora[1] et al pointed out, current adhesive specifications are deficient in specifying adhesive properties. More recently a torsion ring test piece has been used to obtain shear and tensile properties[7-11].

The use in analysis and design, of bulk adhesive properties, is erroneous as the adhesive system in most structural joints is in the order of thousandths of an inch in thickness. Thin film adhesive properties, are in general significantly different than those of the bulk adhesive. Moreover, the effects of "scaling" have been observed in many materials and configurations.

The use of a cylindrical torsion ring test piece can provide adhesive shear property data of typical bonded joint thickness, but requires extreme care in loading to insure a pure torque only. Additionally, the cost per test item is quite high and the specimen configuration is notably different from the geometrical configuration in which the adhesive is used as a structural element.

An alternate approach, namely the thick adherend symmetric lap joint, has been proposed[12,13,14] as a viable specimen with

which to obtain the effective thin film adhesive shear modulus, proportional limit stress and ultimate shear strength. Obtaining adhesive properties from this test, provides data readily usable in the numerous methods of analysis in use today, for determining stresses and deformations in both the adhesive and adherends of bonded joints. Further, the trends associated with cogent variables such as adhesive thickness, surface roughness, ply orientation, temperature, residual strains due to curing and strain rate for various adhesive systems, can be obtained through these standardized tests.

The objective of this research is to look in depth at the proposed shear specimen in an attempt to determine its usefulness in obtaining the desired adhesive properties. To do this, one must address several questions. Is the specimen a reliable and accurate means of characterizing the behavior of the adhesive when restrained by two "rigid" adherends? If so, what are the constraints within which the test should be run?

To answer these basic questions, a comprehensive theoretical and experimental effort has been formulated. A closed form analysis of the joint, a series of tests to check the accuracy of the analysis, a parametric study to determine the optimum specimen parameters, a critical review of the measurement systems used and the results of several adhesive tests are presented.

B. ANALYTICAL STUDY

To gain insight into the linear-elastic response of a

symmetric lap joint specimen, subjected to an axisymmetric load, a comprehensive method of analysis is presented. General relations for the stress couple, transverse shear resultant and in-plane stress resultant at any location in the adherends is derived. Use of these relations and the appropriate boundary conditions enables one to predict accurately the state of stress in both the joint adhesive material as well as at any point in the adherends. A full-field experimental verification of the analytical model is also shown. The analysis assumes the joint to be composed of generally orthotropic adherends secured with an isotropic adhesive. A plane strain approach (i.e. the panel is assumed to be infinitely wide in the width direction), incorporating the effects of transverse shear, normal strain, and thermal effects is taken. The analysis consists of the solution of two fourth order ordinary homogeneous differential equations. The state of stress in the adhesive is shown to generally consist of shear and normal stresses with the shear stress becoming zero at the free edges of the overlap.

C. FORMULATION OF THE PROBLEM

Given two identical rectangular panels of generally orthotropic material; each sheet has length ($L_1 + L_2$) and thicknesses (h_1 and h_2). The thickness of the adhesive (η) is small compared to (h_1) and (h_2). The far ends of the sheet are supported and are loaded in tension by a force of (T) lbs/unit width, Figure (8A). The structure is divided into four elements for ease of analysis, (Figure 8B). The theory to develop the general relations for the

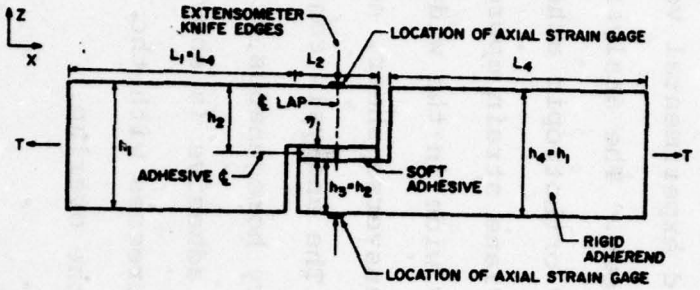
Z
X
EXTENSOMETER KNIFE EDGES
LOCATION OF AXIAL STRAIN GAGE
$L_1 = L_3$
L_2
L_4
℄ LAP
h_2
η
T
h_1
ADHESIVE ℄
$h_3 = h_2$
SOFT ADHESIVE
$h_4 = h_1$
T
RIGID ADHEREND
LOCATION OF AXIAL STRAIN GAGE

FIGURE 8A

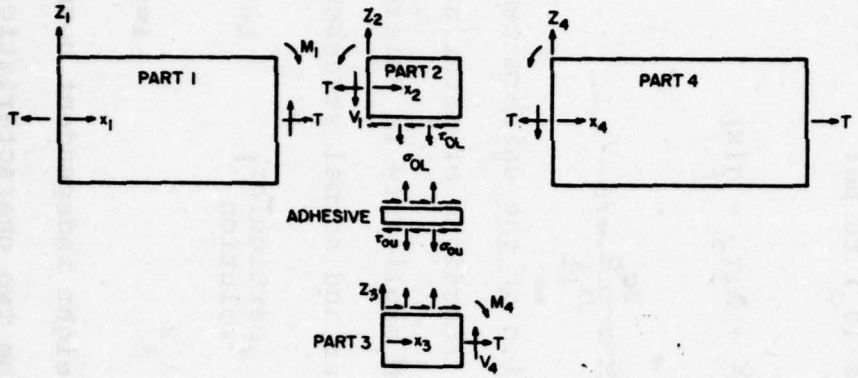
Z1
PART 1
T
x1
T
M1
Z2
PART 2
T
x2
V1
τOL
σOL
ADHESIVE
τOU
σOU
Z4
PART 4
T
x4
T
Z3
M4
PART 3
x3
T
V4

FIGURE 8B

stress couple, in-plane stress resultant, transverse shear resultant and governing differential equations for the adhesive shear stress is quite lengthy and is presented in explicit detail in References [7,8].

Assuming that Parts (2) and (3) are identical, Reference [8] shows the governing equations for the adhesive shear stress (τ_o) and normal stress (σ_o) to be:

$$A_1 \frac{d^4\tau_o}{dx^4} + A_2 \frac{d^2\tau_o}{dx^2} + A_3\tau_o = g(x) \tag{1}$$

$$B_4 \frac{d^4\sigma_o}{dx^4} + B_5 \frac{d^2\sigma_o}{dx^2} - \frac{2\sigma_o}{D_{11}} = 0 \tag{2}$$

where g(x) is a function of the uniform temperature distribution and all constants are functions of material properties and geometry and are given explicitly in Reference [8].

The adhesive shear and normal stresses are of the form:

$$\tau_o(x) = S_i e^{\lambda_i x} + \left(\begin{matrix}\text{particular}\\ \text{solution}\end{matrix}\right) \qquad i=1,4 \tag{3}$$

$$\sigma_o(x) = -\beta_i\lambda_i S_i e^{\lambda_i x} \qquad i=5,8 \tag{4}$$

where the S_i are the eight independent boundary value constants, λ_i are the roots of the two characteristic equations, and β_i is a function of (A_1-A_3) and λ_i.

Numerical values for S_i are determined by inspection of Figure (8B). They are:

$$\tau_o(x_2=0) = \tau_o(x_2=L_2) = 0 \tag{5}$$

and

$$@\ x_2 = 0\ ;\quad M_2(o) = M_1\ ;\quad T_2(o) = T$$

$$M_3(o) = T_3(o) = V_2(o) = V_3(o) = 0 \tag{6}$$

$$N(x)_2^T = g_1(o)\ ;\ N(x)_3^T = g_2(o)$$

$$@\ x_2 = L_2\ ;\quad M_3(L_2) = M_4\ ;\quad T_3(L_2) = T$$

$$V_3(L_2) = V_2(L_2) = T_2(L_2) = M_2(L_2) = 0 \tag{7}$$

$$N(x)_2^T = g_1(L_2)\ ;\quad N(x)_3^T = g_2(L_2)$$

Reference [8] shows that $M_1 = -M_4 = -(\frac{h_1}{2} - \frac{h_2}{2})T$ and that $V_1 = V_4 = 0$. $N(x)_i^T$ is the axial load induced by thermal effects.

Figure (9) displays the adhesive stress distribution in the symmetric lap joint. The dashed lines refer to a typical stress distribution one may anticipate if the specimen is improperly designed. This is primarily due to the disconcerting effect the specimen feels when the geometry and material properties of the specimen are mismatched. The result is the formation of significant stress concentrations at the ends of the overlap and an accompanying non-uniform shear stress state along the overlap length. A properly designed specimen's adhesive stress distribution is given by the solid lines in Figure (9).

D. EXPERIMENTAL CONFIRMATION

To facilitate a confidence in the analytical model and in turn its capacity for designing an optimum shear modulus specimen, both full-field photoelastic and strain gage tests were performed. PSM-1 photoelastic material with a fringe value of 40 psi-in, a Young's Modulus of 340,000 psi, and a Poisson's

FIGURE 9

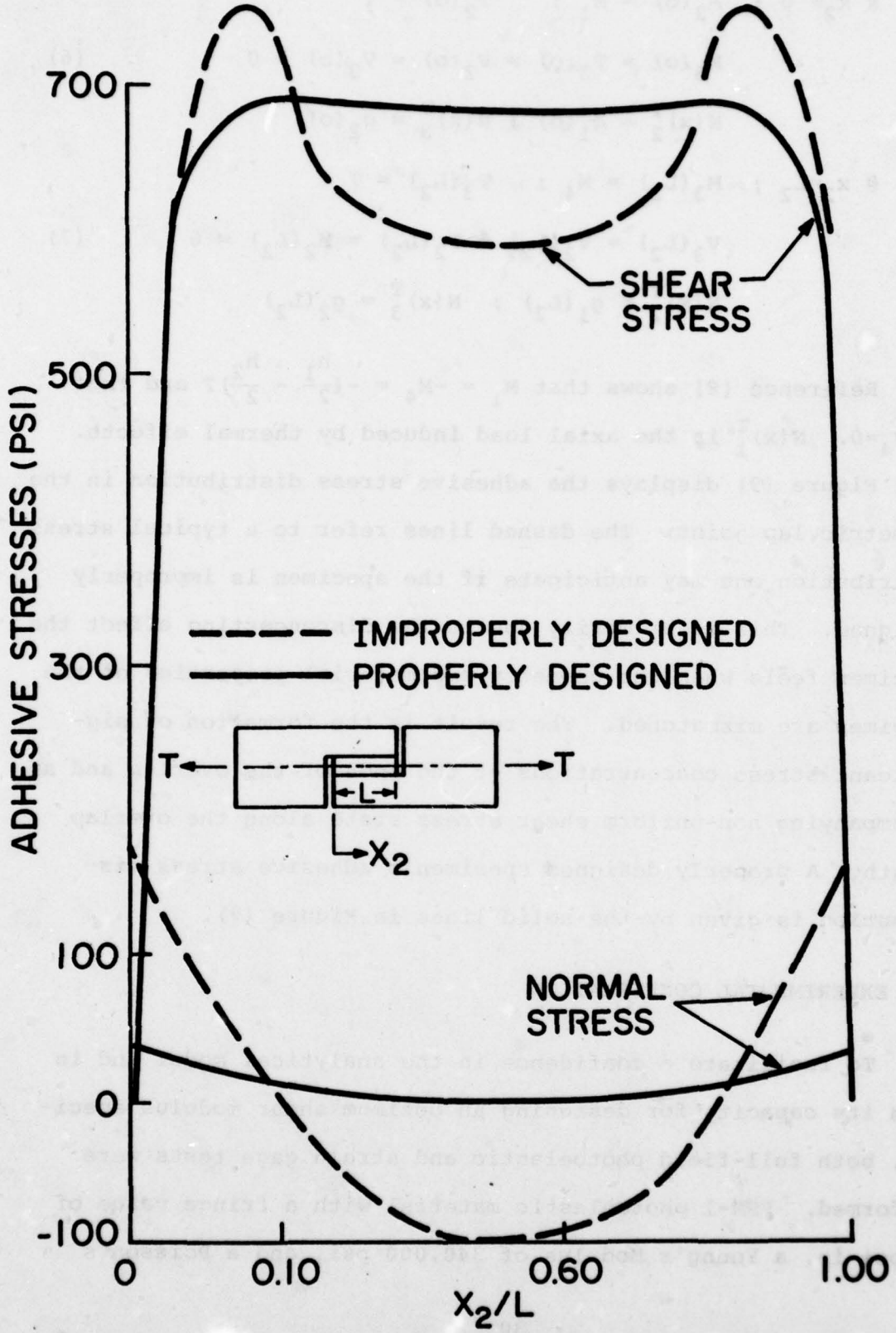
700
500
300
100
0
-100
ADHESIVE STRESSES (PSI)
SHEAR STRESS
IMPROPERLY DESIGNED
PROPERLY DESIGNED
T
T
L
X2
NORMAL STRESS
0
0.10
0.60
1.00
X2/L

ratio of .38 was used to model the joint. A typical photoelastic model and its dimensions are shown in Figure (10). Sheet thickness was .25". To facilitate a comparison between the experimental and analytical approaches, the photoelastic specimens pertinent dimensions and material properties were input into the analytical routine. Results are reduced to field plots of the isochromatics shown in Figure (11). Excellent correlation is seen to exist between the two models. However, correlation was not as good when the gap to H_2 ratio was appreciably less than one. This is directly the result of the Saint Venant effect coming to the fore, whereby the load is physically introduced into the overlap area in a significantly different manner than that prescribed by the analytical model. This effect should be considered in the design of an optimum test specimen.

An additional verification of the analytical model was made by mounting .032 inch gage length axial strain gages on the outer adherend surfaces of three 7075-T6 aluminum and four 1002-S fiberglass specimens, (Figure 8). The adhesive was EA951. The strain gage readings reflect the strain due to the axial load and compressive moment. The tests were conducted at ambient temperature, 20-30 percent humidity and at a crosshead rate of .02 in/min in an Instron tensile tester.

A summary of the test results and the accompanying theoretical predictions are given in Table (4). The strain readings represent an average value of strain over the gage length. For comparison purposes, the theoretical strain values are taken at the location of the centerline of the actual gages.

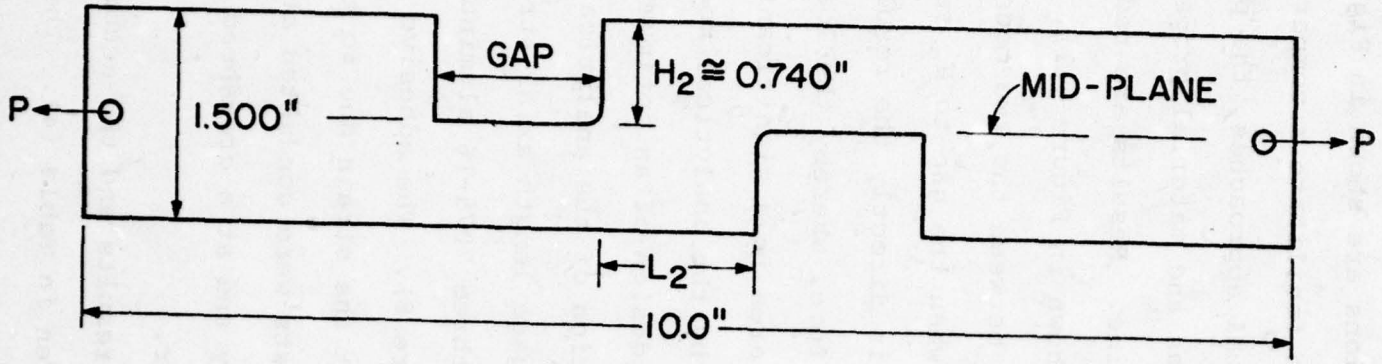

FIGURE 10

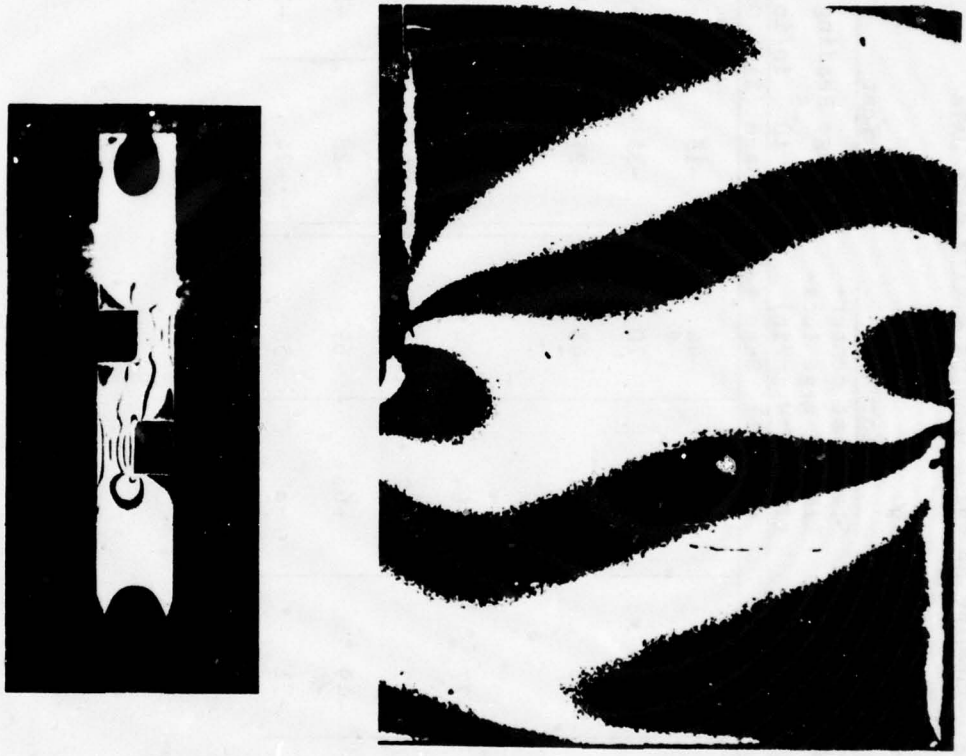

FIGURE 11

TABLE 4. SUMMARY OF SHEAR MODULUS STRAIN GAGE DATA

Spec. No.	L_1* (in)	L_2 (in)	h_1** (in)	T=220 lb. Test: Gage Reading x 10^{-6} in/in		T=220 lb. Theory: Strain at centerline of gage location (10^{-6} in/in)		T=110 lb. Test: Gage Reading x 10^{-6} in/in		T=110 lb. Theory: Strain at centerline of gage location (10^{-6} in/in)	
				Gage (1)	Gage (2)	Gage (1)	Gage (2)	Gage (1)	Gage (2)	Gage (1)	Gage (2)
7075-T6-1	4.390	.265	.510	-71	-38	-88	-44	-18	-25	-22	-45
-2	4.390	.281	.509	-73	-67	-80	-70	-35	-35	-33	-33
-4	4.465	.453	.897	-23	-33	-42	-45	-27	-52	-30	-45
L002-S Glass-1	4.568	.275	.534	-70	-77	-64	-64	-37	-24	-30	-30
-2	4.552	.265	.534	-64	-42	-62	-50	-31	-19	-31	-20
-4	4.217	.703	.516	-50	-49	-65	-69	-28	-27	-34	-32
-5	4.217	.687	.516	-51	-51	-65	-58	-24	-24	-30	-30

* See Figure (8)

** $h_2 \cong .50\ h_1$

Width of specimens $\cong$ 1.0"

Judging the adequacy of the analytical model by use of strain gages in this instance is somewhat sensitive as one is trying to compare very small strain readings. Generally minor errors like gage transverse sensitivity, variation in material properties, and sensitivity of the measurement circuitry can be significant in this region of strain measurement. Discrepancies of 10-20 micro-inches are not unreasonable. Therefore, after consideration of these effects and the reproducibility of the test data as seen from inspection of Table (4), the authenticity of the analytical model would seem to be justified again.

E. OPTIMUM SPECIMEN DESIGN

Having ascertained the validity of the analytical model, it becomes desirable to determine the optimum geometry for test specimens composed of various adherend-adhesive material combinations. In conjunction with this, it is also desirable to define the constraints, if any, for the accurate implementation of such a test.

Such a study was undertaken. The pertinent parameters were effective shear modulus, lap length, thickness of the adherend, and the primary modulus (Q_{11}) of the material. As many adhesives are isotropic and possess a Poisson's ratio close to 1/2, the effective tensile modulus was assumed to be three times the effective shear modulus. In this way the maximum adverse normal stress effect was realized.

For this study, the constraints governing the selection of

the optimum specimen geometry are:

1. the variation in shear stress (deformation) in the adhesive over ± 37.5% of the overlap length measured from the centerline of the joint should be ≤ 10 psi (uniform).
2. the normal stresses in the adhesive should be minimized especially in the central area of the joint.
3. if measurement of the adhesive shear modulus and proportional limit are to be made using a device attached to the adherends outer surface, (point A in Figure 5), it should be placed at the joint centerline thereby minimizing the bending error introduced along the overlap.

Evaluation of the parametric results dictates that one understand the kinematics of the surface measurement system presently in use in responding to the specimen when loaded. Only then can one understand the errors inherent in using such a test to obtain the adhesive effective shear modulus and the proportional limit shear stress, with a properly designed specimen.

Figure (12) defines the kinematical relations that exist during a test. As is readily evident, while the adhesive may deform uniformly (A'A'), the inability to have perfectly rigid adherends introduces an error attributable to moment relief (A'A"). Therefore, the surface measurement system may record a significant bending deformation error unless the moment effects in each adherend (AA") offset each other. This is only

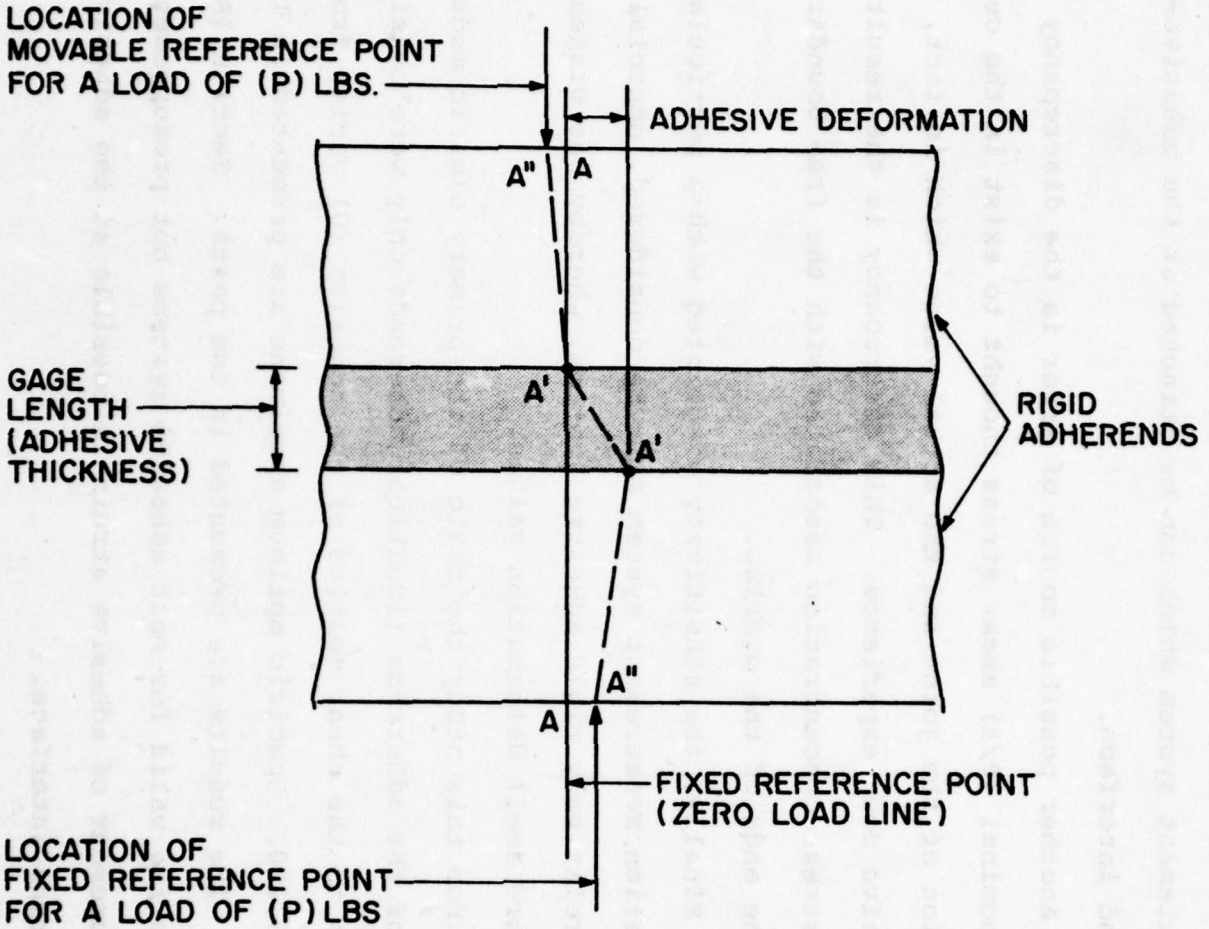

Figure 12 Schematic of the Kinematics to Measure Adhesive Displacement at Adherend's Surface.

the case at the center of the overlap region of the joint. Therefore, the location of the measurement system is all important. Moreover, it emphasizes the desirability to develop a measurement system which can be attached at the adhesive-adherend interface.

Another possible source of error is the discrepancy between the nominal (P/A) shear stress thought to exist in the central portion of the joint and the actual value which in fact, the adhesive does experience. This discrepancy is the result of the stress concentration associated with the free boundaries at the ends of the overlap.

Finally, the sensitivity associated with a particular deformation measurement system must be considered, especially for relatively rigid adhesive systems, whereby one wishes to measure small deformation values.

For this study the ratio of the primary elastic modulus (E) of the adherends (identical adherends only were considered) to the shear modulus of the adhesive (G) varied from 38 to 36,250. Specific optimum specimens are presented in Table (5). The results are presented in two parts. Section (A) results are valid for most adhesive systems but presupposes that measurement of adhesive strain is possible at the adhesive-adherend interface.

Figure (13) shows the percent error in measurement of the true adhesive deformation vs. placement of a measuring device along the adhesive-adherend interface. Within the inner 75 percent of the overlap length the error is a maximum of three

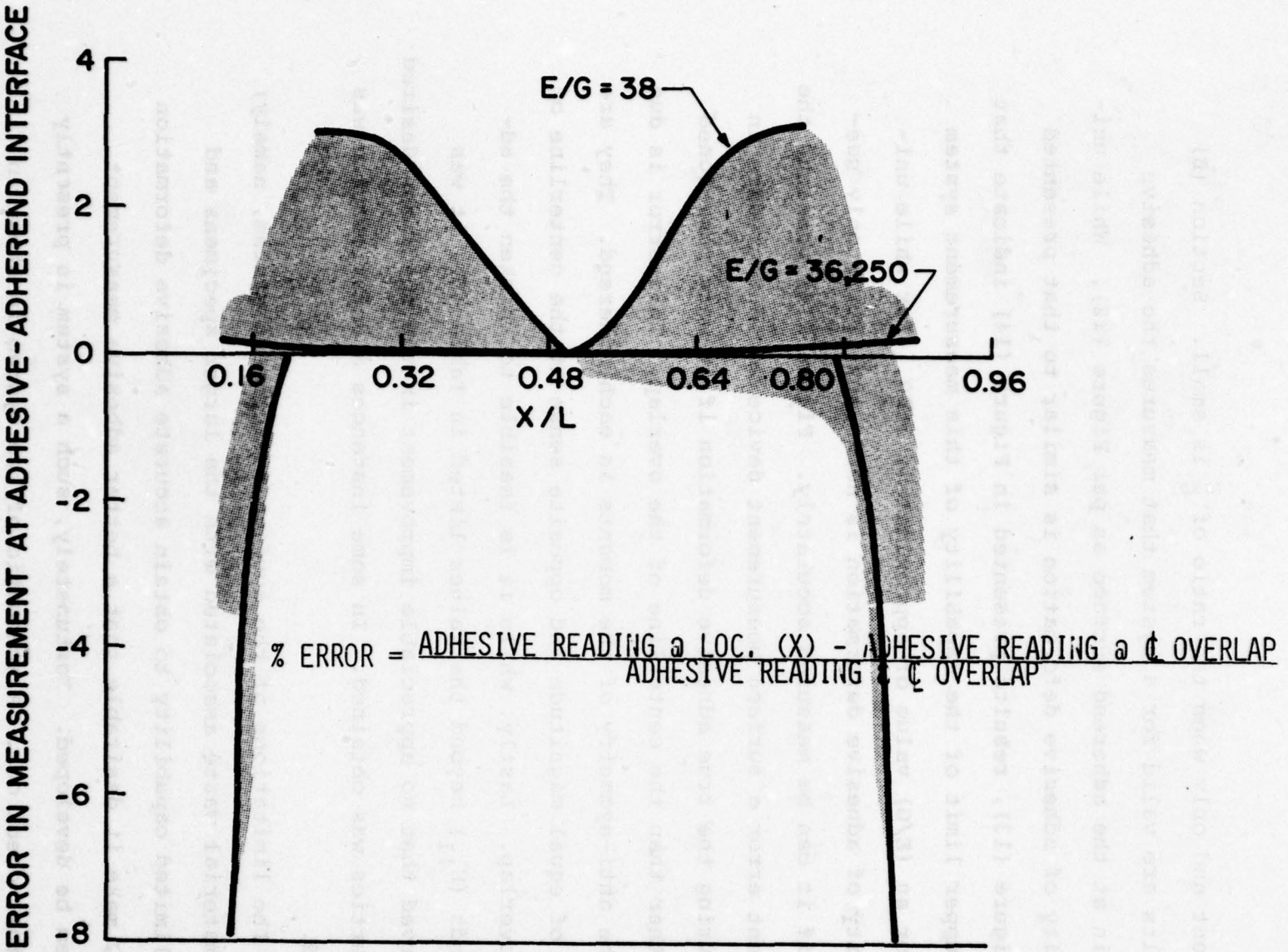

FIGURE 13 PERCENT ERROR IN MEASUREMENT OF THE TRUE ADHESIVE DEFORMATION VS. $(\frac{X}{L})$ LOCATION OF MEASUREMENT DEVICE FOR ADHESIVE SPECIMENS.

percent and only when the ratio of $\frac{E}{G}$ is small. Section (B) results are valid for a system that measures the adhesive strain at the adherend surface as per Figure (12). While uniformity of adhesive deformation is similar to that presented in Figure (13), results presented in Figure (14) indicate that the upper limit of the capability of this measurement system is for an (E/G) value of approximately 2000. For while uniformity of adhesive deformation is necessary, it is only useful if it can be measured accurately. Figure (14) presents the percent error a surface measurement device would introduce in measuring the true adhesive deformation if it were positioned at other than the centerline of the overlap. This error is due to the anti-symmetry of the moments in each adherend. They are only of equal magnitude and opposite sense at the centerline of the overlap. Lastly, while it is feasible to thicken the adherends (H_{11}) beyond the values listed in Table (5), it was observed that no appreciable improvement in the specimens desired properties was obtained. In some instances a deterioration was noted.

The limitations of the surface measurement system, namely; the material waste associated with the larger specimens and its limited capability to obtain accurate adhesive deformation data, make it desirable that a better adhesive measurement system be developed. Fortunately, such a system is presently in final check out. A schematic of the system is shown in Figure (15). Fundamentally, it uses a three point pick-up on each side of the specimen. It is attached at the adhesive-adherend

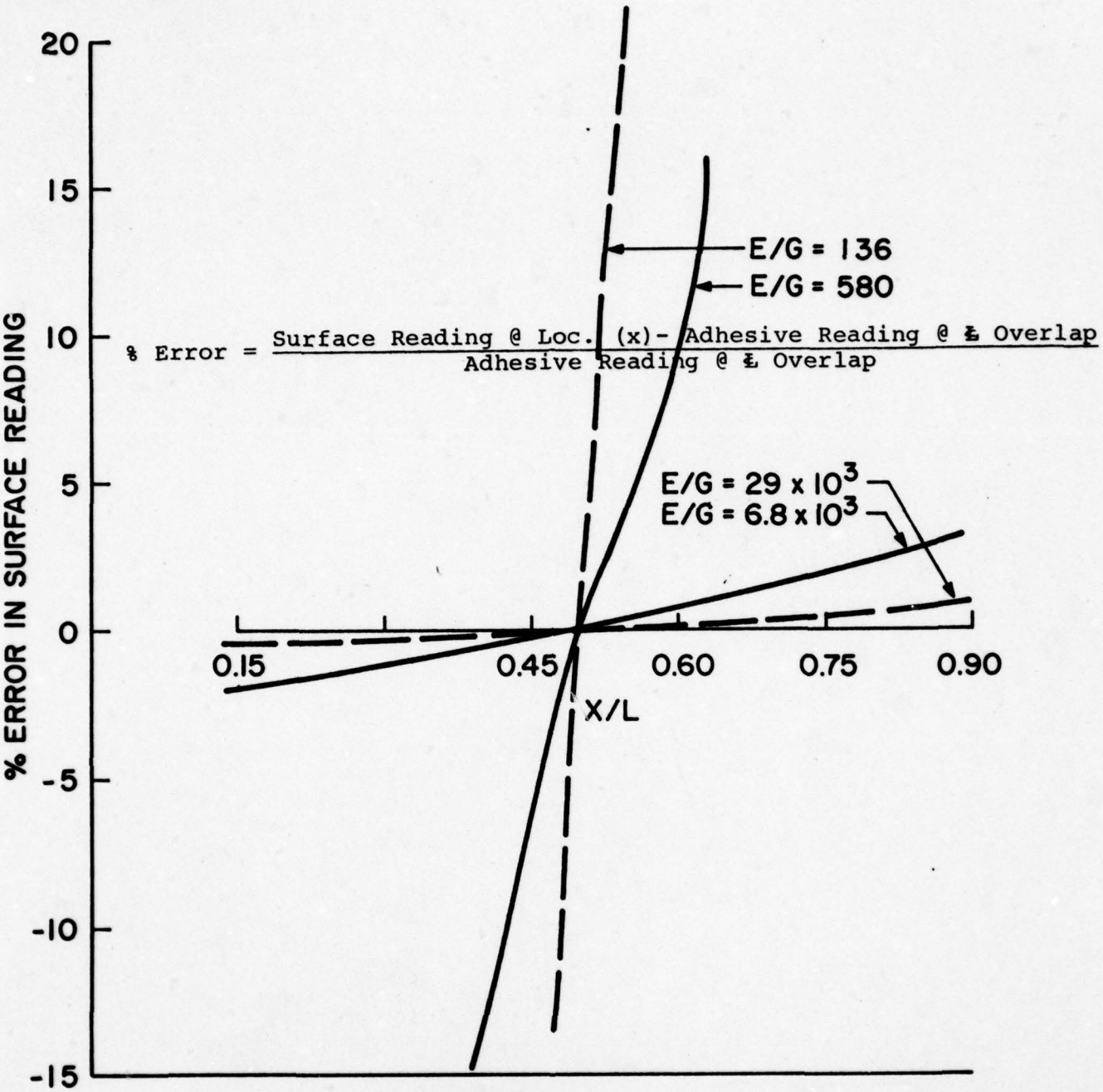

Figure 14 Percent Error in Measurement of True Adhesive Deformation vs. Location of Knife Edges Along Adherend Surface.

TABLE 5. SUMMARY - OPTIMUM SHEAR SPECIMENS

A.) ADHESIVE MEASUREMENT SPECIMENS

Primary Elastic Modulus (x 10^6 psi)	H_1* (in)	L_2 (in)	Range of Usage In Terms of Adhesive Modulus Factor (C_s)*** ($\times 10^6$ lb/in^3)
6.8	.75	.50	Full Range
10.3	.75	.36	" "
16.0	.75	.36	" "
29.0	.75	.36	" "

B.) ADHEREND SURFACE MEASUREMENT SPECIMENS

Primary Elastic Modulus (x 10^6 psi)	H_1* (in)	L_2 (in)	Range of Usage In Terms of Adhesive Modulus Factor (C_s)*** ($\times 10^6$ lb/in^3)
6.8	.75	.40	.20→6.0
6.8	1.50	.88**	6.0→25.0
10.3	.90	.40	.20→6.0
10.3	2.50	1.30	6.0→25.0
16.0	.90	.40	.20→6.0
16.0	2.50	1.30	6.0→25.0
29.0	.90	.40	.20→6.0
29.0	2.50	1.30	6.0→25.0

* Refers to dimension shown in Figure (8).

** No optimum found.

*** $C_s = \frac{\text{Shear Modulus (psi)}}{\text{Adhesive Thickness (in)}}$

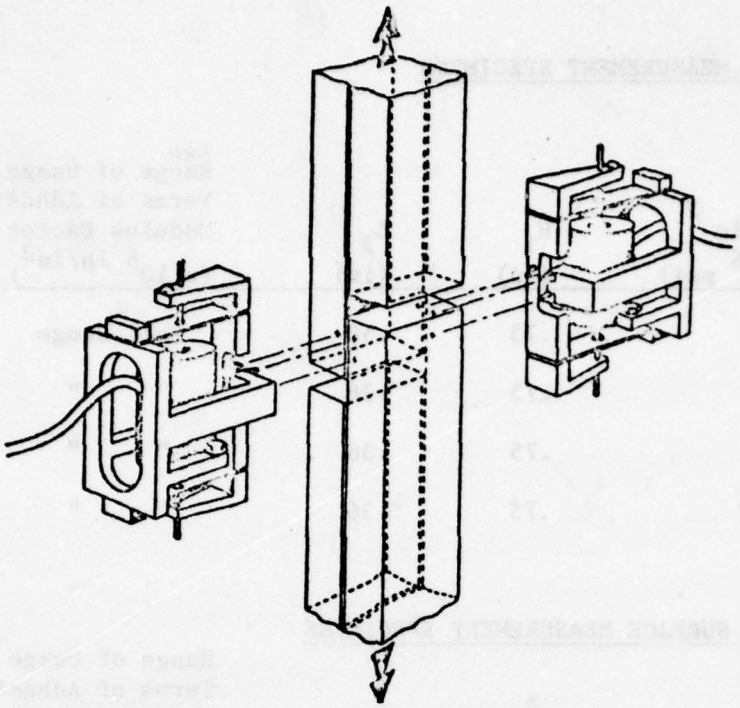

Figure (15) New Adhesive Deformation Measurement Device

interface. The net effect is to cancel out adherend deformation effects while giving an average adhesive deformation reading.

Further details of the system can be obtained from Mr. Ray Kreiger of the American Cyanamid Company of Havre de Grace, Maryland.

The effective thin film shear modulus ($G_{eff.}$) of the adhesive can be calculated per equation (9).

$$G_{eff.} = \frac{(\text{Load})(\text{adhesive thickness})}{(\text{Surf. Area})(\text{adhesive deformation})} \quad (\text{Stress Factor}) \qquad (9)$$

Again, results of the parametric study indicate that a stress factor correction, Figure (16) must be included in the

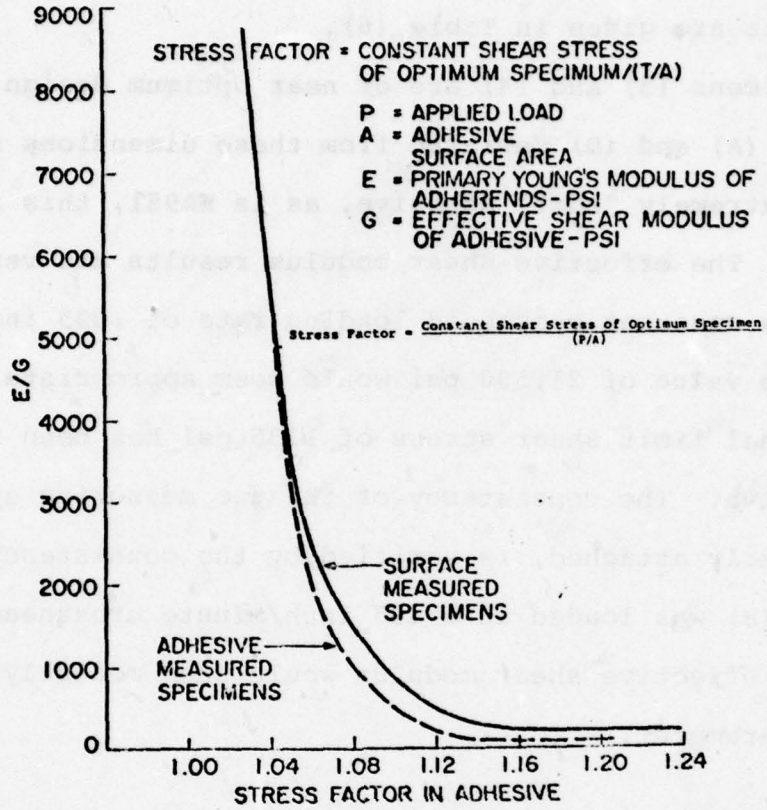

Figure (16) Stress Factor vs. E/G

calculation of the effective shear modulus. This factor accounts for the fact that the shear stress is at a uniform level other than the nominal (P/A) stress level. Additionally, the proportional limit shear stress which is obtained from the load-deformation plot should also be adjusted by the stress factor.

F. EXPERIMENTAL RESULTS

Both the surface measurement system described earlier and the adhesive measurement system shown in Figure (15) were used to obtain the effective shear modulus of EA951 nylon-epoxy

adhesive in a series of screening tests. Pertinent geometry and results are given in Table (6).

Specimens (3) and (4) are of near optimum design while specimens (A) and (B) deviated from these dimensions somewhat. With an extremely "soft" adhesive, as is EA951, this is permissible. The effective shear modulus results are very consistent for a constant crosshead loading rate of .005 inches/minute. An average value of 21,500 psi would seem appropriate, while a proportional limit shear stress of 1235 psi has been recorded for the adhesive. The consistency of the two measuring systems, when properly attached, is verified by the consistency of results. Specimen (B) was loaded at a .05 inch/minute crosshead rate. In turn, the effective shear modulus would seem modestly dependent on this parameter.

G. CONCLUSIONS

An analytical methodology with subsequent experimental verification has been presented for the proper design of the symmetric lap joint test item. Optimum specimen design for various adhesive-adherend combinations is presented. Also, a discussion on the difficulties of measuring a true adhesive "effective" modulus and a new approach to solving this problem are presented.

As is readily evident, much additional work on adhesive characterization needs to be done. Both improvement of measuring techniques and the response of various adhesives to environmental and load rate parameters should be ascertained.

TABLE (6) SUMMARY OF SHEAR TEST RESULTS

Spec.	H_1 (in)	L_2 (in)	Adhes. Thick (in)	Deformation @ 220# ($\times 10^{-6}$ in)	S.F.	G Eff (psi)	P.L. Stress (psi)	Ult Stress=P/A (psi)	Type Failure
3	.897	.453	.00763	163.	1.1150	22000.	1242.	5209.	adhes.-cohes
4***	.897	.446	.00642	169.	1.0957	20270.	1227.	5290.	adhes.-cohes
A	.500	.336	.01030	350.	0.9520	21600.	-	6776.	cohes.-adhes
**B	.510	.298	.00790	240.	1.0100	24138.	-	6890.	adhes.-cohes

* All data results average of (3) tests, crosshead rate .005 in/min

** Crosshead rate = .05 in/min

*** Used Kreiger system of Fig. 15.

EA951 Adhesive - 7075-T6 adherends, width $\simeq$ 1.00 in., room temp.- 15% rel. hum.

ABSTRACT

The results of an experimental program are given which provides quantitative and reproducible shear property data for many of the present and promising adhesives for use in bonded joints in composite material structures.

The experiments employ a composite material test specimen in which the adhesive material is in a film configuration, typical of bonded joints, rather than measuring bulk adhesive properties. Because both the flexural and in-plane stiffnesses of the glass-epoxy adherends of the test piece are extremely large ($>10^6$) compared to a parameter proportional to the shear and extensional modulus of the adhesive film, the adhesive film is virtually in a state of constant shear stress with negligible normal stresses. The details of the shear test piece have been published previously.

The adhesives tested were those recommended by the major adhesive manufacturers, those selected by NASA Langley in the civil aviation program and those utilized in the USAF PABST program.

The data reported includes the ultimate shear stress, initial shear modulus, and elongation to failure, both mean values and standard deviations, for specimens made by the adhesive manufacturer and the University of Delaware.

CHAPTER III

SHEAR PROPERTIES OF PROMISING ADHESIVES FOR BONDED JOINTS IN COMPOSITE MATERIAL STRUCTURES

B. INTRODUCTION

For several years, research has been conducted toward the goals of being able to determine accurately the stresses and deformations in both the adhesive and the adherends of bonded composite material structures, subjected to static, dynamic, and thermal loads, including the very important effects of combined high temperature and high relative humidity termed "hygrothermal."[15,16] Accurate methods of analysis were developed which analyze the stresses and deformations in both the adhesive and adherends in panels bonded together in a single lap joint configuration, subjected to a uniaxial in-plane panel loading.[13,17,18] These methods of analysis were found to be quite accurate.[5] Subsequently, these methods were used to conduct parametric studies to determine the relative effects of altering all geometric and material property variables.[19,20] More recently, these methods have been improved and extended to include hygrothermal effects, in a form that can be utilized for many joint configurations.[16] In order to determine the stresses in both adhesive and adherend, it is necessary to determine the mechanical properties of the adhesive materials utilized. In particular, the stress-strain curve of the adhesive materials must be known to know the effective moduli, yield strengths, ultimate strengths and elongations to failure of the adhesive materials in shear, tension and compression.[17] Not only should these properties be determined for each temperature and humidity combination, but they should be obtained through test pieces which employ the

adhesive in a film or bond configuration, i.e., a test piece that has nearly the same surface area to volume ratio as the adhesive in a typical joint configuration, rather than obtaining bulk form adhesive mechanical properties. Proper shear test and tension test pieces have been developed in this program.[17] The shear test specimen will be discussed herein. It differs from existing ASTM standards[21] because they utilize thin, metal adherends in a simple lap configuration, and a shorter joint length.

The methods of analyses derived through this program are elastic only. The hypothesis that in a fatigue environment, the maximum stress anywhere in the adhesive at the mean load level should be at or below the proportional limit of the adhesive material to successfully withstand a "runout" of 4×10^6 cycles has been confirmed experimentally through more than a hundred tension-tension fatigue tests employing glass adherends and Hysol EA951 and EA9628 adhesives, at room temperature and low humidity, and mostly with the stress ratio R = +0.1.[22,23,24]

Recently conducted research provides a comparative study of the mechanical properties at room temperature and low relative humidity of various adhesive systems employing the standard shear test specimen developed during this program.[14] Shear tests at 212°F were also conducted. That temperature corresponds to the utilization of the adhesive in a Mach 2 vehicle.[25]

Inclusive descriptions of research of others in adhesive bonded joints are readily available.[13,17,26,29]

C. EXPERIMENTAL PROGRAM

The shear test specimen utilized is shown in Figure 1. It is the same test piece designed and utilized earlier in the research program. The design results in both the flexural and in-plane stiffness of the adherend being millions of times larger than a parameter proportional to the shear stiffness and extensional stiffness of the adhesive film, namely,[13,17,18,30]

$$\frac{D_{11}}{E_{eff}\eta^3} > 10^7 \tag{1}$$

$$\frac{A_{11}}{G_{eff}\eta} > 10^6 \tag{2}$$

where D_{11} adherend flexural stiffness in longitudinal direction

A_{11} adherend in-plane stiffness in longitudinal direction

E_{eff} adhesive tensile modulus

G_{eff} adhesive shear modulus

η adhesive film thickness

Because of this, the shear stress over the length of the bond is virtually constant, except for it going to zero over a very small but measurable region at each end of the adhesive bond line. Obviously, the shear stress in the adhesive must be exactly zero at each end because it is a free surface. That fact was not accounted for in the earlier, more simplified analyses of Goland and Reissner.[3]

Also because of this design, the normal stresses in the adhesive (those normal to the load, or the peel stresses) are

virtually zero due to negligible specimen rotation during loading because of the very stiff adherends.

Thus, through this design the shear stress in the adhesive can accurately be calculated as the applied load divided by the planform area of the adhesive film.

The tests are conducted by aligning the shear test specimen, Figure 8A, in the jaws of a static tensile test machine. Then, a zero length extensometer, in this case a Tinius - Olsen Model S-1000-2 LVDT, is attached such that the knife edges are aligned exactly normal to the load at the midpoint of the adhesive bond line. Because of the specimen design, in which the extensional stiffness of the adherend is millions of times larger than the adhesive shear modulus parameter, any relative axial displacement measured by the extensometer is due to shear deformation in the adhesive film.

Because the shear stresses are virtually constant over the length of the bond line, hence, so are the shear strains, ε, defined here as the relative axial displacement of the extensometer, δ, divided by the adhesive bond line thickness, η.

In the test program, the bond line thickness is measured at the midpoint on each side of the 1" wide specimen and then averaged to give the adhesive thickness, η.

The following approach was used to identify the promising adhesive systems. Each of the major adhesive manufacturers was contacted for their recommendations as to the best structural adhesives they could suggest. In all cases recommendations were offered, bonding procedures given, and in most cases, samples of

the adhesive material were provided gratuitously. In addition, NASA-Langley provided valuable recommendations concerning the adhesives being used in their commercial aircraft program. Likewise, we were aware of the adhesive systems being utilized in the Air Force PABST program.[28,29] Most of the adhesives utilized in the NASA and PABST programs were included in this test program. Hopefully, therefore, all of the promising adhesive systems have been characterized herein.

Manufacturing facilities for making the shear test specimens are available at the University of Delaware, and those specimens fabricated strictly adhered to the procedures and practices suggested or specified by the adhesive manufacturer. As a check, each adhesive manufacturer was requested to fabricate a group of six specimens in order that we could determine whether the U. of D. manufactured specimens were statistically identical to the specimens manufactured by the adhesive manufacturer.

In either case, specimens were manufactured from bonding two 11" x 7" plates of 3M glass-epoxy spring stock, 1/4" thick, together. After proper bonding, a machined groove was cut in the 7" direction, see Figure 1, 1/4" wide down through one of the 1/4" adherends and through the adhesive bond lines. Secondly, the plates were inverted and a corresponding milling procedure was used at a distance 1" away from the previous operation to provide an adhesive test length of 1". Lastly, the plates were cut parallel to the 11" direction, such that from the 7" wide plates, six 1" wide test specimens result. Finally,

measurements of the bond line thickness are made photographically with a Bausch & Lomb Balphot Metallograph, as discussed earlier, the length of the bond line is measured, as well as the width of the adherends.

It is noted that the bond line thickness depends solely on the adhesive material used, and the bonding procedures prescribed by the manufacturer. Shims or other artificial means of maintaining bond line thickness prevent the application of prescribed pressure, and thus are unacceptable. In spite of the variations in bond line thickness, the reproducibility of test results is excellent.

D. TEST RESULTS

All the adhesives tested are listed in Table 1, not in any specified order.

It should be noted that XB-163K is the 3M replacement for their AF55. One material utilized in the NASA Langley program is the Cavalon, and the materials used in the PABST program include AF55 (now replaced by XB-163K), and the EA9628.

In Table 7, mean values of the ultimate shear strength, τ, the effective shear modulus, G_{eff}, and the ultimate shear strain, $\varepsilon = \delta/\eta$, as defined earlier, are given. Also included are the standard deviations associated with each mean value, and the number of tests performed. In each case, the specimens tested include those fabricated by the manufacturer and also by the U. of D., except for those which are asterisked, signifying that only U. of D. fabricated specimens were tested. In each case the

Table 7

	Manufacturer	No. of Specimens	τ	G_{eff}	ε
1	Conap DPAD-5633	5	1460/84	1065/213	1.748/.396
2	Conap AD-3	6	2065/98	3130/1015	1.883/.300
3	3M AF-30	12	2256/260	2004/530	2.644/.387
4	3M XB-163K	12	2458/261	2189/744	2.136/.809
5	3M AF-143	11	2173/192	3092/1325	1.543/.661
6	3M AF-147	11	2476/118	2954/983	1.714/.673
7	Mobay Mondur CB-75	11	1791/187	761/240	6.052/2.457
8	Mobay Mondur MR	17	2341/202	2180/1584	4.161/3.368
9	Mobay Mondur PF	12	2329/87	1867/1179	>4.639
10*	Atlas Amphesive 801	3	1229/102	6089/382	.328/.051
11*	Atlas Epoxy Bond Paste	3	711/27	4288/1034	.380/.052
12*	Hysol EA-9628	6	3011/198	2138/380	>1.931
13*	Hysol EA-9320	6	2746/95	5577/947	.626/.181
14*	Hysol ADX-663	6	3003/251	1945/667	>2.398
15*	Adhesive Engineering Aerobond 3000	4	928/183	2972/932	.447/.129
16*	Adhesive Engineering Aerobond 2185	6	2195/249	1536/284	-
17*	Adhesive Engineering Aerobond 2143	5	1800/55	11,084/766	>.281
18*	Dupont Cavalon 3200S	3	1091/265	1699/294	.959/.153
19	Dupont Cavalon 3000	6	1576/148	574/62	3.238/.583

ultimate strengths of both the manufacturer and U. of D. specimens indicate that they come from the same statistical population, based upon the mean values and standard deviations calculated.

It is seen that for many of the adhesives, the measured ultimate strains are greater than one. When the strains are large, the shear stress value, τ, should be regarded only as the applied load per unit adhesive film area, because the adhesive in that case is not in a state of pure shear.

The effective shear modulus is the initial slope measured below the proportional limit.

From Table 7, it is seen that the strongest adhesives in shear are the Hysol EA 9628 and the ADX-663, while the lowest value is that of the Atlas Epoxy Bond Paste.

The stiffest adhesive by far is the Adhesive Engineering Aerobond 2143 adhesive, while the least stiff is the Cavalon 3000. The most ductile adhesive is the Mobay Mondur CB-75, and the most brittle is the Atlas Amphesive 801.

It is noted that most of the ultimate strength values have standard deviations considerably less than 10% of the mean values, and only a few exceed that percentage. Looking at the failure surfaces of specimens fabricated either by the supplier or by the U. of D., some failures are cohesive, some are adhesive failures, none were adherend failures. The low values of standard deviation indicate little influence of cohesive or adhesive type failure. As would be expected the standard deviations are relatively larger for the effective modulus values and the ultimate strains.

In Figures 17 and 18 are plotted the averaged values of shear stress vs. strain curves for 18 of the adhesives tested. The ordinate is τ, which in the linear elastic range can be aptly called the shear stress, and in the nonlinear range should be considered only as the axial load divided by the planform area of the adhesive film, as discussed earlier. Likewise, the absissa, ε, is the axial displacement of the extensometer, δ, divided by the adhesive thickness, η. The method used to plot the data in Figures 2, 3 and 4 involves the use of the cubic spline,[21] an innovative procedure which insures the curve goes through each data point measured. In the case here the curve goes through the average of the samples at each load level the displacements were measured.

Table 8 provides data analogous to Table 1 for selected adhesives at 212°F, after the specimens had come to constant temperature, and at low relative humidity. It is seen that the strongest adhesives are Hysol ADX-663 and EA9628, which were the strongest at room temperature.

Again, the stiffest, by far, is the Adhesive Engineering Aerobond 3000, and it was by far the most brittle. The 3M AF-147 was the least stiff and the most ductile of those tested.

Again, all standard deviations on strength values are low, being less than 8% for the ductile adhesives and less than 12% for the brittle Adhesive Engineering Aerobond 3000. Once more the standard deviations are higher for both the shear modulus and the strain to failure.

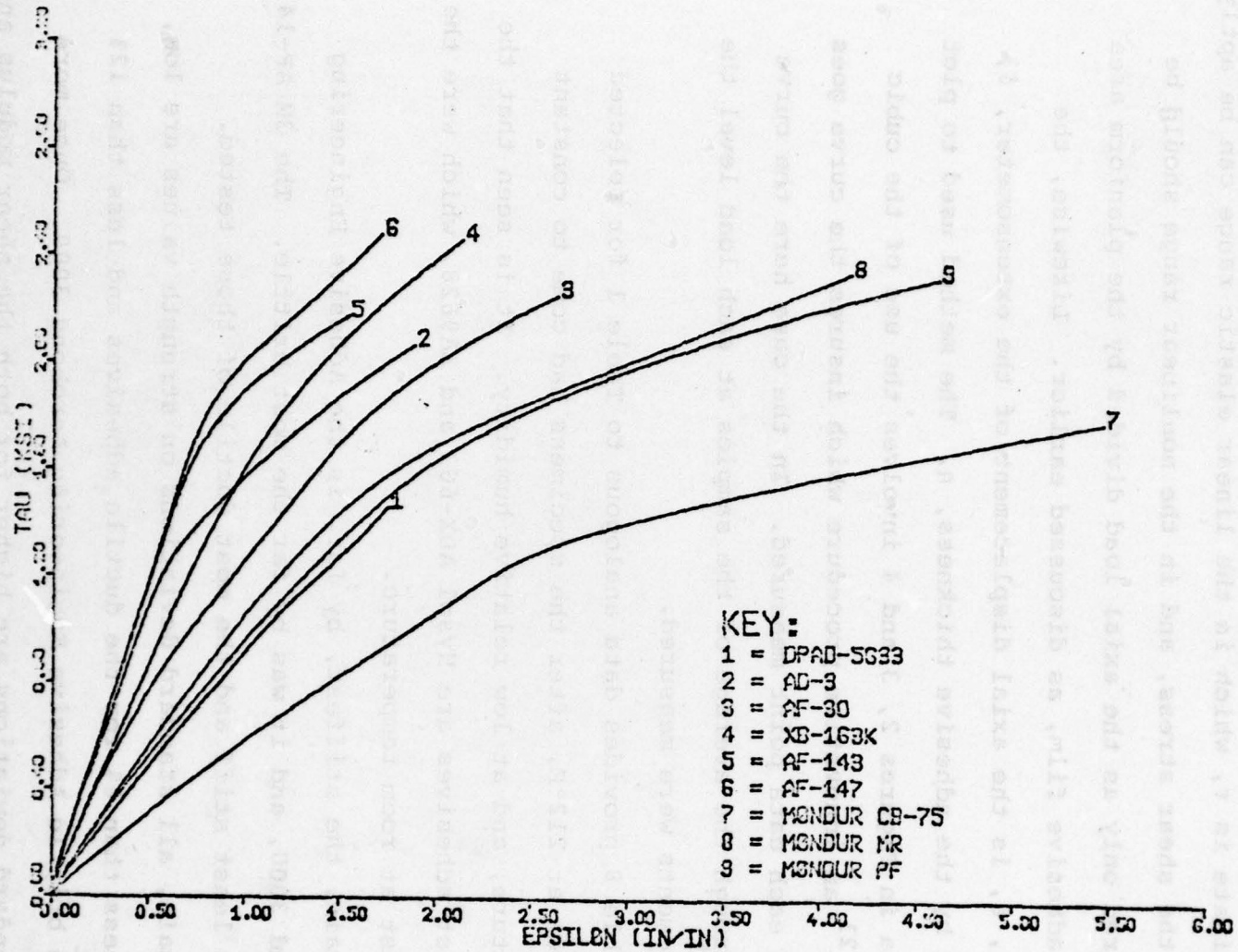

FIG. 17- ADHESIVE SHEAR STRESS-STRAIN CURVES, 70°F

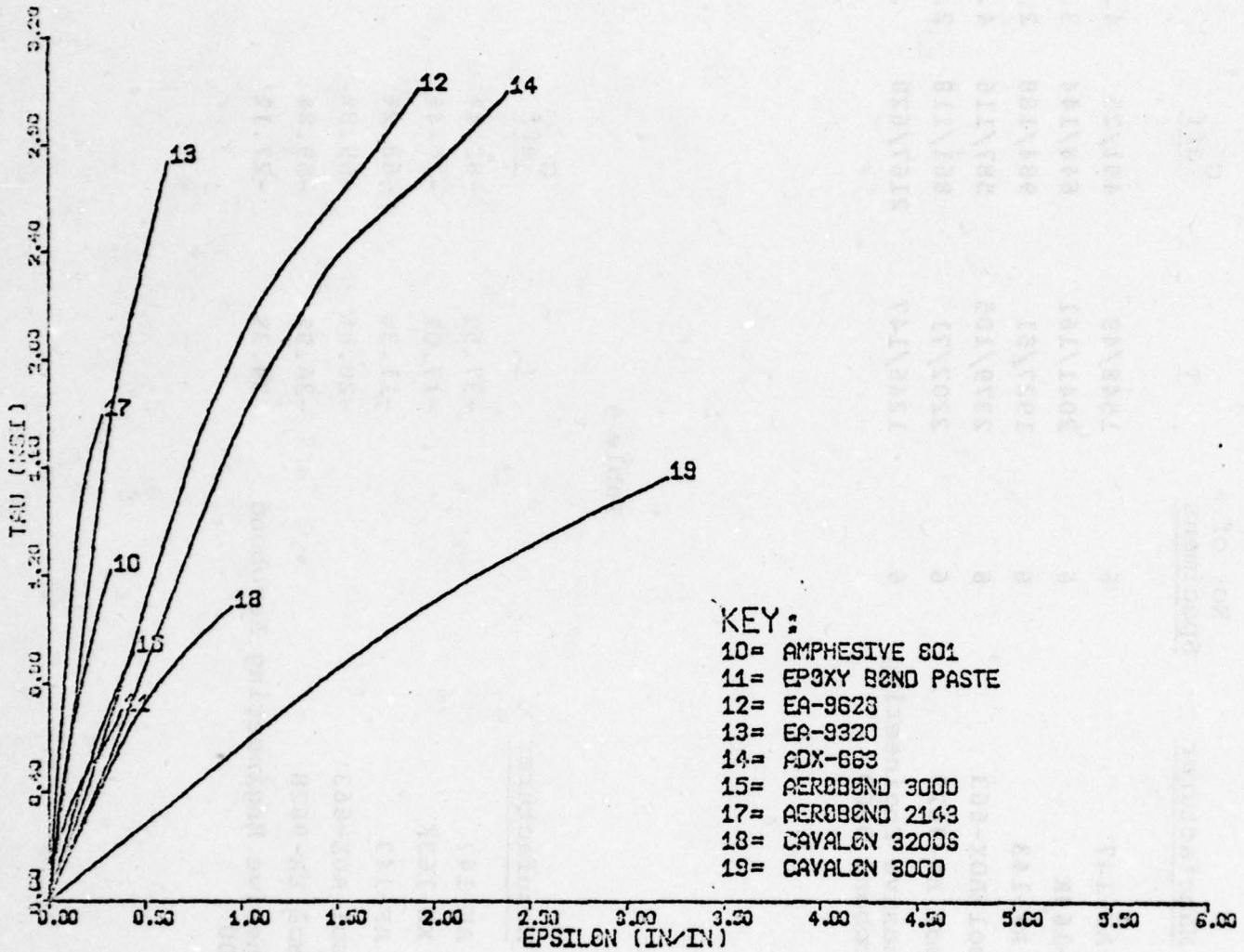

FIG. 18 ADHESIVE SHEAR STRESS-STRAIN CURVES, 70°F

Table 8

Manufacturer	No. of Specimens	τ	G_{eff}	ε
1* 3M AF-147	6	1548/49	491/25	4.292/.711
2* XB-163K	6	2041/161	648/144	3.770/.469
3* 3M AF-143	6	1927/51	984/188	2.282/.278
4* Hysol ADX-663	6	2379/105	587/116	4.263/.644
5* Hysol EA-9628	6	2202/71	861/118	2.578/.365
6* Adhesive Engineering Aerobond 3000	6	1246/147	2167/628	.769/.277

Table 9

Manufacturer	τ	G_{eff}	ε
3M AF-147	-37.5%	-83.4%	150.4%
3M XB-163K	-17.0%	-70.4%	76.5%
3M AF-143	-11.3%	-68.2%	47.9%
Hysol ADX-663	-20.8%	-69.8%	<77.8%
Hysol EA-9628	-26.9%	-59.8%	<33.5%
Adhesive Engineering Aerobond 3000	34.3%	-27.1%	72%

Figure 19 is a plot of the average values of shear stress as a function of strain for the dry adhesives at 212°F, in which it is seen that the total strain energy to failure is considerably more for Hysol ADX-663 than for the other adhesives tested.

Table 9 shows a comparison of each mean value of shear stress at failure, shear modulus, and strain at failure between the value at 212°F and the value at 70°F. It is seen that while the percent reduction in strength is in the order of 10-40%, the reduction in stiffness is considerably greater, as is the increase in strain to failure.

E. CONCLUSIONS

First of all, the overall reproducibility of the ultimate strength results (i.e., the low standard deviations) lends confidence to the test, the testing method, and to the usability of the adhesives systems tested in routine manufacturing environments.

The Hysol EA-9628 and ADX-663 are the strongest of the 19 adhesives tested, while the Adhesive Engineering Aerobond 2143 is the stiffest adhesive in shear, and the Mobay Mondur CB-75 is the most ductile material.

At 212°F the two Hysol adhesives, ADX-663 and EA-9628 are the strongest tested, the Adhesive Engineering Aerobond 3000 is the stiffest tested, and the adhesive with the largest strain energy to failure is the Hysol ADX-663.

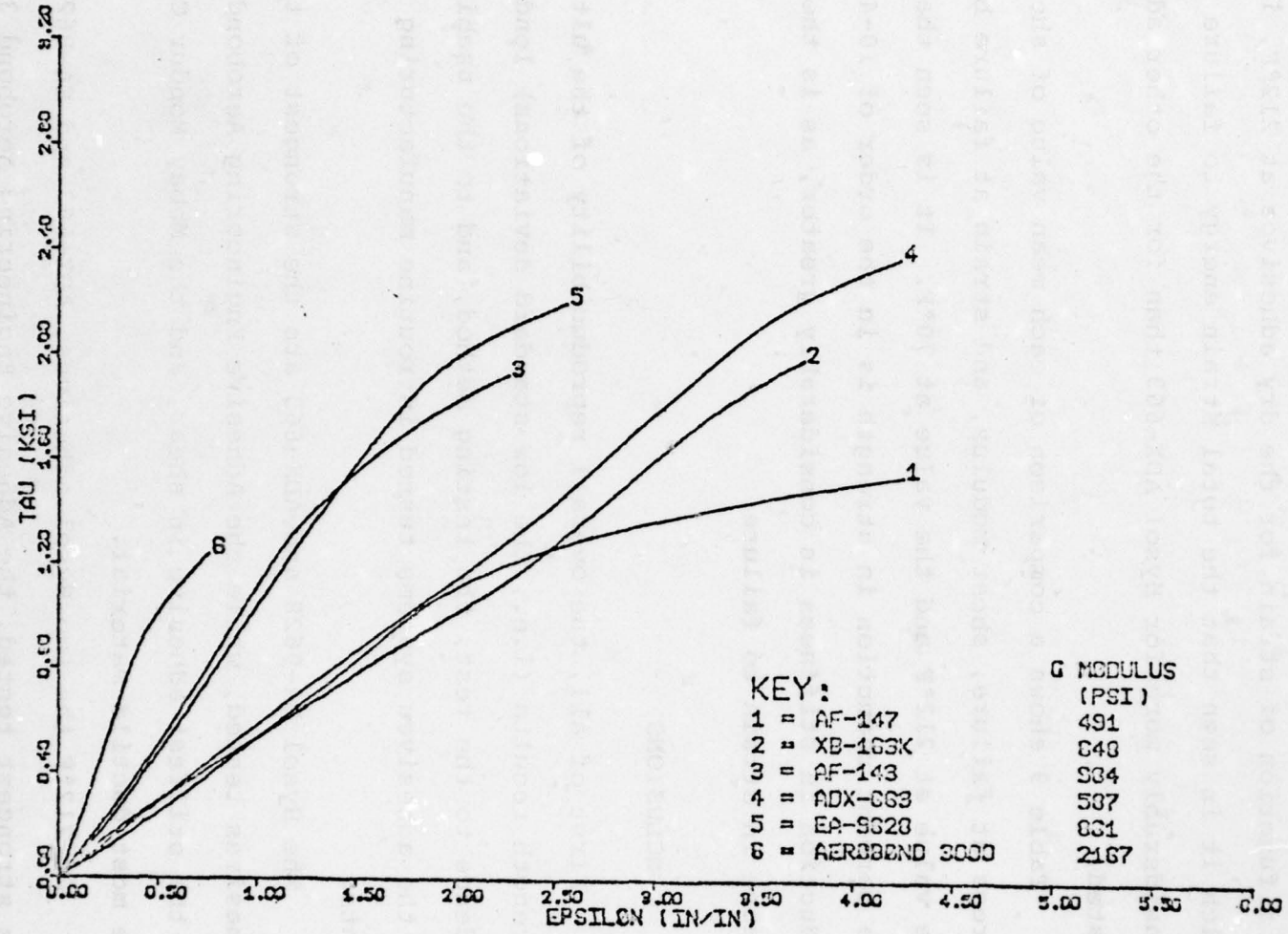

FIG.19- ADHESIVE SHEAR STRESS-STRAIN CURVES, 212°F

F. ACKNOWLEDGEMENTS

The authors wish to express their appreciation to Ralf Tschirschnitz, Laboratory Supervisor, for his assistance; Kenneth Baldwin, Composite Specialist, for manufacturing the U. of D. test pieces; and John Valentine, a student, for his assistance in data reduction.

Likewise the authors express their appreciation to Richard A. Pride, Head, Composites Section, NASA-Langley for his suggestions of promising adhesive systems.

Finally, the authors would like to express their appreciation to the following for suggesting adhesive materials, fabrication procedures, samples of adhesive materials, and fabricated panels for testing: (the order of listing is arbitrary) Ron Cornell, Conap, Incorporated, Olean, New York; E. C. Valentine and M. Kennedy, The 3M Company, St. Paul, Minnesota; John H. Kaiser, Jr., Atlas Minerals, ESB, Inc., Martztown, Pennsylvania; W. Warrach and G. J. Schexnayder, Mobay Chemical Corporation, Pittsburgh, Pennsylvania; W. C. Williams, Hysol Division, Dexter Corporation, Pittsburgh, California; Frank L. Kelley, Hexcel Corporation, Belair, Maryland; John T. Mizulo, Adhesive Engineering Company, San Carlos, California, D. W. Metzger, E. I. duPont de Nemours & Company, Wilmington, Delaware.

REFERENCE LIST

1. Mylonas, C. A. and N. A. de Bruyne, "Adhesion and Adhesives", First Ed. N. A. de Bruyneand, R. Houwink, Eds. Elseiver, Amsterdam 1951, p. 96.

2. Cherry, B. W. and Harrison, N. L., "The Optimum Profile for a Lap Joint", Journal of Adhesion, Vol. 2, April 1970, pp. 125-128.

3. Goland, M. and Reissner, E., "The Stresses in Cemented Joints", Journal of Applied Mechanics, March 1944.

4. Wang, Douglas Y., "Influence of Stress Distribution on Fatigue Strength of Adhesive - Bonded Joints", Experimental Mechanics, June 1964.

5. Sharpe, Jr., W. N. and Muha, Jr., T. J., "Comparison of Theoretical and Experimental Shear Stress in the Adhesive Layer of a Lap Joint Model," Proceedings of the Army Symposium on Solid Mechanics, 1974,: "The Role of Mechanics in Design - Structural Joints," AMMRC MS 74-8, September 1974.

6. Zabora, R. F., et al., "Adhesive Property Phenomena and Test Techniques", AD729873, July, 1971.

7. Hughes, Edward J. and Rutherford, John L., "Study of Micromechanical Properties of Adhesive Bonded Joints", Technical Report 3744, Aerospace Research Center, General Precision Systems, Inc., Little Falls, New Jersey, August, 1968.

8. McCarvill, W. T. and Bell, J. P., "Torsional Test Method for Adhesive Joints", Journal of Adhesion, Vol. 6, pp. 185-193, 1974.

9. Corvelli, N. and Saleme, E., "Analysis of Bonded Joints", Grumman Aerospace Corporation, Advanced Development Report No. ADR-02-01-70.1, July 1970.

10. Kuenzi, E. W. and Stevens, G. H., "Determination of Mechanical Properties of Adhesives for Use in the Design of Bonded Joints", FPL Report No. 011, September 1963.

11. Lin and Bell, "Effect of Polymer Network Structure Upon the Bond Strength of Epoxy-Aluminum Joints", Journal of Applied Polymer Science, Vol. 16, pp. 1721-1733, 1972.

12. Renton, W. J. and Vinson, J. R., "The Analysis and Design of Composite Material Bonded Joints under Static and Fatigue Loadings," Air Force Office of Scientific Research TR No. 73-0494, August 1973.

13. Renton, W. J. and Vinson, J. R., "The Analysis and Design of Anisotropic Bonded Joints," Air Force Office of Scientific Research TR No. 75-0125, August 1974.

14. Renton, W. J. and Vinson, J. R., "Shear Property Measurements of Adhesives in Composite Material Bonded Joints," A.S.T.M. Composites Reliability Conference, April 1974, STP-580.

15. Pipes, R. B., Vinson, J. R., and Chou, T. W., "On the Hygrothermal Response of Laminated Composite Systems, Journal of Composite Materials, pp 130-148, April 1976.

16. Wetherhold, R. C., "An Analytical Model for Bonded Joint Analysis in Composite Structures Including Hygrothermal Effects," Master of Mechanical and Aerospace Engineering Thesis, University of Delaware, June 1976; also, U. of Del., Mechanical & Aerospace Engineering Technical Report 198, March 1977.

17. Renton, W. J. and Vinson, J. R., "The Analysis and Design of Composite Material Bonded Joints Under Static and Fatigue Loadings," AFOSR TR 73-1627, August 1973.

18. Renton, W. J. and Vinson, J. R., "Analysis of Adhesively Bonded Joints Between Panels of Composite Materials," Journal of Applied Mechanics, pp 101-106, March 1977.

19. Renton, W. J. and Vinson, J. R., "The Efficient Design of Adhesive Bonded Joints," Journal of Adhesion, Vol. 7, pp 175-193, 1975.

20. Renton, W. J., Pajerowski, J. and Vinson, J. R., "On Improvement in Structural Efficiency of Single Lap Bonded Joints," published in the Transactions of the Fourth Army Materials Technology Conference, Boston, September 1975.

21. ASTM Standard D1002-72, "Strength Properties of Adhesives in Shear by Tension Loading."

22. Renton, W. J. and Vinson, J. R., "On the Behavior of Bonded Joints in Composite Materials Structures," Journal of Engineering Fracture Mechanics, Vol. 7, pp 41-60, 1975.

23. Renton, W. J. and Vinson, J. R., "Fatigue Behavior of Bonded Joints in Composite Materials Structures," AIAA Journal of Aircraft, Vol. 12, No. 5, pp 442-447, May 1975.

24. Renton, W. J. and Vinson, J. R., "Fatigue Response of Anisotropic Adherend Bonded Joints," Proceedings of the Army Symposium on Solid Mechanics, AMMRC.MS-74-8, September 1974.

25. McBee, O. B., McDonnell Aircraft Co., St. Louis, private communication, November 1976.

26. Renton, W. J., "Structural Properties of Adhesives," Quarterly Progress Reports 1-7, Vought Corporation Advanced Technology Center, AFML Contract F33615-76-R-5205, May 1976 to February 1978.

27. Anon., "Fatigue Behaviour of Adhesively Bonded Joints," Quarterly Progress Reports 3-7, General Dynamics Fort Worth Division Materials Research Laboratory, AFML Contract F33615-76-6-5220, January 1977 to March 1978.

28. Anon., "Primary Adhesively Bonded Structure Technology (PABST)," Technical Bulletins 11-17 McDonnell Douglas - Long Beach, USAF Contract F33615-75-6-3016, January 1977 to May 1978.

29. Anon., "Primary Adhesively Bonded Structure Technology (PABST), Phase Ib; Preliminary Design," AFFDL-TR-76-141, December 1976.

30. Renton, W. J., "The Symmetric Lap-Shear Test - What Good Is It?," Experimental Mechanics, November 1976.

31. Schlegel, P. R., "The Cubic Spline - A Curve Fitting Procedure," Ballistic Research Laboratories Report N-1253, July 1964.